Authors response to Reviewer comment 1 (by anonymous Referee)

David Mair[1], Alessandro Lechmann[1], Marco Herwegh[1], Lukas Nibourel[1], Fritz Schlunegger[1]
[1] Institute of Geological Sciences, University of Bern, Baltzerstrasse 1+3, CH-3012 Bern

Correspondence to: David Mair (david.mair@geo.unibe.ch)

Line by line response

Lines 12- 13 : replace Â´n T at deformation ranged from xx: : :Â˙z with : "Deformation temperatures range between xx and xx…"

Response: This has been implemented.

Line 14: either "ductilely" or "in a ductile manner". Here you are using the present tense, on line 13 it's the past

Response: Both errors were corrected as suggested.

Line 21: "NW-striking" is enough

Response: Indeed; changed to "NE striking" to correct also mislabelling.

Line 22: "feature an immense topographic expression": a complex, but not very clear sentence to say "high altitude"?

Response: This has been clarified. (see next 2 comments).

Line 22: replace "SE-NW striking rim" with "NW striking rim"

Response: done.

Line 23: "offset" between what and what?

Response: Offset between the surface elevation. Wording changed to clarify the sentence.

Line 24: replace "the sedimentary" by "its sedimentary" and delete "rocks of the Aar Massif".

Response: Changed as suggested.

Line 28: Helvetics

Response: Error corrected.

Line 29: early stage of what?

Response: Early stage of the Alpine evolution. Sentence was adjusted accordingly.

Line 29: you can decouple from a basement but you cannot decouple from an evolution (at least not in this context).

Response: The Alpine evolution of the Helvetics was decoupled from the Alpine evolution of the massifs basement rocks. The sentence and the following sentence were restructured to correctly convey this message.

Line 32: add a 150 years old reference

Response: There are several works from the late 19th century (i.e.by Escher v. der Linth, 1837; Baltzer, 1880;). They are discussed extensively in the cited references; thus, they are not only cited now, also "references therein" is added to already cited works.

Line 36: later?

Response: Later In the sense of 2nd half of the 20th century. Sentence was restructured to avoid time confusion.

Line 39: delete "which"

Response: Replaced with "that" in order to correct sentence.

Lines 40 to 43: there is no real usable information for the readers here

Response: The sentence lists the main works over the recent years on the deformation and its chronology in the massif, which we feel should be cited in this paragraph, designed to give a brief overview of previous work. We did expand the sentence to specifically provide some information about the methods used by the studies to advance the understanding of the deformation history of the Aar massif.

Line 49: delete "and to fill the knowledge gap".

Response: done.

Line 53: delete "in the field and"

Response: Done; replaced with "on the surface" to clarify that not all samples are from the railway tunnel.

Line 56: Delete "In addition…history"

Response: Followed to make the sentence more concise.

Line 62: Repetition of line 20

Response: The reoccurring part was deleted to avoid redundancy.

Line 66: "in between": not very clear

Response: Clarified by adding "those gneiss units".

Line 68: SW-strike

Response: done.

Line 75: delete "Alpine" and add "of Alpine age" after "metamorphism"

Response: done.

Line 84: Replace "These mechanisms are considered not to…" with " This process does not appear to be"

Response: done.

Line 85: Massif Line 86: add reference at the end of sentence Line 86

Response: Reference was added.

Line 86: what sort of deformation fabric?

Response: We do clarify the phrasing here: The mentioned phase was characterized mainly by thrusting. The sentence now reflects this (see also next comment).

Line 88: the name of the deformation phase is not so interesting if the kinematics of the deformation are not described.

Response: The kinematic description has been added accordingly.

Line 90: "thrusting": nw-vergent?

Response: The top to NW kinematics are now reflected in the sentence.

Line 93: which recumbent fold? Does it have a name? Is it visible in a figure? Any references?

Response: Here, we refer to the recumbent fold that builds the Doldenhorn nappe. We have clarified this point and also added a reference.

Line 95: what is an inverse succession

Response: An inverted stratigraphic succession; now labelled accordingly.

Line 100: I would delete "differential"

Response: Done as suggested.

Line 101: delete "a phase of"

Response: done.

Line 101: strain partitioning": only interesting to know if you describe what is partitioned into what

Response: This has been clarified.

Line 101: "simultaneously with dextral strike-slip": unclear. Is dextral strike slip part of the partitioning?

Response: The strain partitioning occurred between the strike slip and NW thrusting. We have changed the structure of the sentence accordingly.

Lines 103-104: Pfaffenkopf and Oberaar have no references

Response: All references are given at the end of the sentence to avoid giving same references twice within one sentence.

Lines 104-105: delete "the uplift passively rotated". The uplift is not a force… And add "were passively rotated" after "Doldenhorn Nappes".

Response: Done.

Line 108: which type of brittle structures?

Response: This has been specified.

Line 114: not necessary

Response: We see the point and did remove the sentence (and adjusted the next one).

Line 117-118: delete Line

Response: We do not see why this line should be deleted since it provides information about how we have processed the data processing.

Line 120: "only" should be before, not after mapped

Response: Done.

Line 121: delete only

Response: done.

Line 145: basement

Response: corrected.

Line 145: replace "are present as" with "consist of"

Response: done

Line 148: what is a "granodioritic texture"? Magmatic texture?

Response: There has been a mistake in the original draft. Both coarse- and fine-grained textures are granoblastic, for which we apologize. We have corrected the sentence accordingly.

Line 152: delete "see also"

Response: done.

Line 155: evidence

Response: corrected.

Lines 174-176: delete sentence

Response: We agree and have deleted the sentence.

Line 180: brittle shear zone?

Response: Changed to “brittle faults forming along former shear zones” for clarification purposes.

Lines 181-182: “Note that…sediments” doesn’t need to be between parentheses

Response: It has to be. It is intended to point out why we start with SZ2 in the basement. Therefore, we prefer to keep it in parentheses.

Line 182: replace “faulting behavoiur” with kinematics

Response: done.

Line 183: “However” ???

Response: Corrected. The unfitting word “However” was removed.

Line 183: I cannot see the offset of older structures in Fig. 5b

Response: The SZ2 structures are cut in the footwall by the SZ3 thrusts running through the JSW sediments in Fig. 5b. We do find the offset rather illustrative. However, we added also a reference to Fig. 5c as this image also illustrates the cross-cutting relationship.

Line 189: no dot after SZ2

Response: done.

Line 189: “offsets”: this could give you a shear sense? Why is there no shear sense described? Looking at Fig. 6 I do not find the distinction of SZ2 and SZ3 convincing based on the orientation data. The Rottal net shows a possible distinction into two groups based on the different dip, but there aren’t many data and even there it could be one population only. The Trugberg net doesn’t show two”populations” in my view.

Response: The offset could give us a crude information about the shear sense: top to NW for normal faulting and top to SE for reverse faulting. However, we refrain from this since we do not have lineation data for this data set (as the Trugberg set is inferred from remote sensing). For the Rottal we present information about the shear sense for SZ2 (Line 183: “dominantly top to the NW shear senses”). For SZ3 we now added a sentence where we outline the predominantly top NW-directed thrusting. Regarding the distinguishing of SZ2 and SZ3 in the data for Fig. 6.: We did not differentiate the phases based on the orientation only; we rather measured 2 sets of SZ orientation in the field (Rottal) and via remote sensing (Trugberg). We thus distinguished these phases based on the combination of data of various sources. We admit that the orientation net for the Trugberg itself would not warrant a subdivision of 2 phases.

Line 190: “wider”: give an idea

Response: Given in parenthesis.

Line 190: replace “occurred” with “is”

Response: done.

Lines 190-193: any references to figures?

Response: Reference to Fig. 5 was inserted.

Line 193: “kinematics”: you did not say much about it in the last lines (see comment on Line 189)

Response: We acknowledge the need for more clarity. We thus changed the text accordingly. (see response to comment on line 189) and additionally added a shear sense statement. Thus, we now hope to have clearly stated what kinematics each phase is associated with.

Lines 201-204: a verb is missing in this sentence

Response: Corrected by removing the superficial "that"

Line 210: I doubt it...Mapping certainly reveals something, but I guess something else.

Response: The whole sentence is indeed unnecessary and has thus been removed.

Line 213: why "the first"? It was not mentioned that there were many. Is it S1?

Response: In lines 210 to 213 we describe the characteristics of S1 and label it. With this sentence we state that this is the first foliation formed in the sedimentary rocks (as it overprints the bedding but is overprinted by all later structures). We added "(S1)" after mylonitic foliation for clarification purposes

Line 214: what is the spacing of mylonitic foliations? Spacing between shear zones?

Response: We rephrased the sentence to clarify.

Line 217: The reference to Fig. 7c comes after "more than one def phase", but it doesn't show that. It only shows the boudinage.

Response: The reference was misplaced and is moved to the appropriate place in the sentence as we intend to illustrate the impressive boudins made up of dolomites. Yet it still shows minor multiphase deformation.

Line 219: past tense (led) not always used in the text. Reference to maps and figures?

Response: Done.

Line 222: argument for the synchronous development of S1 and SZ1?

Response: We do see that the statement of synchronous development is misplaced here as we give our argument for it in Sect. 5.3.1 in the discussion section. Thus, we replaced it with observations that indicate contemporary formation. (parallel orientation of S1, SZ1 and foliation spacing decreasing towards SZ1).

Line 223: what is the shear sense of these shear zones?

Response: This is difficult to specify due to the later deformation that partly rotated the orientation of the sedimentary stack. We do see a general top to NW trend of shearing and thrusting. We now added an according statement in a sentence to address this and to highlight the thrust nature (see next comment on Line 225).

Line 225: it needs to be stated before that these shear zones are thrusts. And what displacement direction?

Response: Done (see also previous comment).

Line 225: "of" the footwall rather than "in"?

Response: Corrected.

Line 227: subsequent to what?

Response: Here, we refer to the phase of thrusting (SZ1) and the contemporaneous formation of S1, which constitutes deformation stage 1 in our framework; the text was adjusted accordingly.

Line 228: what is a rotated sigma clast? And…why does a rotated sigma clast indicate rotation of the initial structures? And… what deformation phase causes an anticlockwise rotation of some 50, looking East? "As a result": of something that is not really explained.

Response: Misleading sentence in our previous version. Rotation is documented by rotated textures (i.e. bedding in competent units) within sigma clasts along with rotation and folding of S1 parallel veins. The rotation we discuss in this context occurs in section view looking east (not in map view). We rewrote the corresponding paragraph to clarify these points.

Line 229: what are EN and EW?

Response: Some regions in which the structural data was collected. This was clarified and references to Figs. 2 & 9 were added.

Line 230: "This deformation stage": I am lost. Which one? The one that rotated the fabrics? What are the kinematics of this deformation?

Response: The second stage rotated preexisting structures by local folding (see also response to comment on Line 231). We rewrote the corresponding paragraph for clarification purposes. We also added a kinematic description.

Line 230: how do you know it is not preserved?

Response: We realized that our original statement was confusing and not really needed so we removed it to increase conciseness and clarity.

Line 231: "and the folding": so this deformation phase is the folding? What axial plane and fold axes orientation?

Response: This deformation is characterized in the sediments by local folding near the basement cover contact, and it intensified towards the SE (= towards the more internal). Steep SE dipping axial planes and SW/W to NE/E striking folding axis are dominant, but they can be locally complex and chaotic. We now explicitly state this in the rewritten paragraph (see also responses to comments on Lines 228 & 230).

Line 233: "Subsequent NW directed shearing": not easy to understand and visualize and I cannot really see it in Fig. 11b that is quoted at the end of the sentence. Where do I see the flat-lying limbs? What is the evidence for a subsequent NW-directed shearing in the first place?

Response: The reference to Fig. 11b is incorrect, instead Fig. 10a is now correctly referenced. We further added several references to Fig. 7 to illustrate our points. We do see several thrusts that offset S1, S2 and SZ1 and therefore had to occur later (see. Figs. 2,10,11c). These thrusts are the reason we see basement rocks in the summit region of the Eiger-, Moench and Jungfrau summit, right on top of Mesozoic sediments. Along these thrusts the S3 foliation intensifies, and we measured a swath of stretching lineations on S3-parallel slip planes with top to NW shear sense (Fig. 9). We have adjusted the text to clarify this (see also the newly added Figs. 10a,b and the next responses to comments on Line 234).

Line 234: "now": do you think the limbs were initially steep?

Response: We do think that the limbs formed as intermediate-steep SE imbricate stack by fault propagation folds. The subsequent folding and thrusting led to their current flat lying position in the frontal part and folds in the internal SE part.

Line 234: this observation of the result should be described by a photo or sketch of the structures, not by a schematic recap of the Discussion/Conclusions.

Response: We agree and added new Figures to illustrate specifically the cross-cutting and overprinting relations of key structures (now Figs. 10a,b).

Line 234-235: S3? How can one distinguish S3 from S2 that are sometimes parallel?

Response: S3 formed sometimes (not always) parallel to S1 (not S2!). Often S3 foliation and SZ3 thrusts cut S1 with a small angle, yet sometimes the form at a very high angle to each other (as illustrated in Figs. 7a,b). This usually occurs when S1 structures were rotated during the phase forming S2 structures. S3 structures have a similar orientation and a shared SE to NW evolution. This evolution is characterized by SE dipping in the SE to flat and slightly NW plunging in the NW (Figs. 10,11). We adjusted the text of the whole section to better describe these observations. We also added the new Figures (10b,c) to further document the cross-cutting and the incorporation of basement slivers at different stages.

Line 236: difficult to follow. Why is it really necessary to distinguish an S3 from an S2 here?

Response: We actually distinguish S3 from S1. S1 is folded by stage 2 deformation that produced a weak S2 axial plane foliation. Both are cut by S3 structures.

Line 237: which one is the "same" orientation?

Response: We intend to mention that S3 features a fairly 'consistent' orientation throughout the study area; see response to comments on Lines 234-235.

Lines 210-240: not easy to follow, especially the mixture of orientation with cross-cutting relationships and of microstructural characteristics.

Response: We saw the need to rephrase the entire paragraph for clarification purposes.

Line 243: what does oblique mean here? Kinematics of these faults?

Response: Oblique refers to the general orientation of the faults as well as the shear sense (strike slip with reverse/normal fault behavior). We amended the text to reflect that.

Line 258: specify and justify the geothermal gradient used for the conversion of T in depth

Response: We use a uniform averaged geothermal gradient of 27 °C km^{-1} for the upper crust as often given with a range of 25° to 30° C km^{-1} for the continental lithospheric crust (Pollack and Chapman, 1977). It seems reasonable for the youngest exposure history of the Aar massif (~26-28 °C km^{-1}; Valla et al., 2016; Schlunegger and Willett, 1999) and is close to the inference by Glotzbach et al. (2010) of 25 °C km^{-1}. The reason for the depth estimation was to highlight the rather shallow position during peak T of Alpine deformation (especially compared to southern Aar massif; Herwegh et al., 2017). We recalculated the depth estimation for the given gradient of 27° C km^{-1} and added statements in in the main text to address this properly with 3 new references.

Line 266: evidence for being deformed as an "ensemble"?

Response: They share the same deformation fabric, same RSCM peak temperature, which we describe in Sect. 4.2.2 (as it is now referenced in the sentence). We have clarified this point.

Line 267: consistent? With what?

Response: Internally consistent. Sentence was changed accordingly.

Line 268: less shortening: evidence? Quantified?

Response: We did not (yet) quantify the individual offset along strike, but gave a qualitative statement based on the map view. We added a statement to clarify this point.

Lines 269-270: why?

Response: The steepening occurred mostly during SZ2, due to the large differential block uplift in the basement (SZ2) that passively steepened the sedimentary cover in the SE. A statement was added to clarify this.

Line 272: The cover-sediment interface?

Response: We wrote “cover sediments” which we rephrased to “sedimentary cover” to avoid possible confusions.

Line 283: why “already”?

Response: No need for this; deleted.

Line 284: has this wedging been described before in the text? Wedging associated with folding? I am lost…

Response: This particular wedging-in refers to a pre-Alpine event, which we take from literature survey. An additional reference was added, where an up-to-date and extensive discussion of this Pre-Alpine evolution is presented. We want to highlight the already existing structures before the Mesozoic.

Line 286: evolution of what?

Response: The pre-Alpine basement gneisses. Sentence was amended accordingly.

Line 289: succeeding???

Response: changed to Alpine.

Line 293: favorable for what?

Response: for localization of Jurassic normal faults. Sentence was adjusted to clarify.

Lines 295-301: I am not sure why these observations are important in the context of the results session and of the paper.

Response: We do generally find the relative consistency of the strata remarkable. We briefly discuss the main trends in the stratigraphy that allows us to differentiate tectonic from stratigraphic features of the map (Fig. 2). We consider this brief section essential for our understanding of how we can differentiate and map the different tectonic slivers.

Lines 302-305: why to mention an own stratigraphic model here that was not presented in the results?

Response: We do present a stratigraphic model in the Appendix A and discuss the main findings in Sect. 4.1.2. The reason for giving the details in the Appendix is that for almost the entire stratigraphic units we confirm previous field data, thus there is not much new insight. Yet most references are quite old, and literature spans several decades, leading often to different and outdated interpretations. Furthermore, there is no consistent and up-to-date stratigraphic model for the region. We thus saw the need to conduct such a compilation (see also previous 2 comments).

Lines 305-307: I am still not sure about the importance of these lines.

Response: See previous 3 comments and responses, respectively.

Line 311: Substratum T constrained by RSCM?

Response: Since the sedimentary cover is still in place on top of the substratum, the inferred Alpine RSCM temperatures are also constraining the T in the underlying basement. We added “Alpine” to the sentence to clarify that we explicitly address the shared peak T.

Line 311: why to give an upper limit to calcite thermometry and mention calcite thermometry at all?

Response: The sentence was misleading. It should convey that the upper temperature constraint is given by the RSCM at around ~320 °C. We rephrased the sentence to clearly state that now.

Line 314: ok, but you should also quote the lower T suggested by XX and White. I think it must be Burkhard, 1993, not Burkhard, 1990.

Response: Done. We adapted the lower boundary to the lower boundary suggested by Kennedy & White (2001) and reference the work. Burkhard reference was corrected.

Line 322-323: repetition of line 317

Response: Very similar indeed. To avoid redundancy and increase conciseness we removed the last 2 sentences of the paragraph (see also comment and response below).

Line 323: well, I am not sure that this can be constrained. The only thing that can be said is that T of 270°C was attained following the recrystallization T inferred by Stipp et al., 2001. What is known about the T peak anyway?

Response: Indeed, we can only constrain the formation to the T window of <330 °C to 270 °C. Since from our data we do not have chronological constraints, we cannot state how close (or not) to peak T the deformation occurred. Therefore, we removed the last sentence.

Line 325: pelitic

Response: Corrected.

Line 325: synchronously: what is the evidence?

Response: We see a parallel orientation of S1 and SZ1; both share the same response to the later deformation (i.e. being cut or modulated by local folding). The evidence for the synchronous formation is now presented with more clarity in Sect. 4.2. and Figs. 10a,b.

Line 326: delete "rheological"

Response: done.

Line 333: was it quantified? What is the evidence?

Response: It was not quantified by retro-deformation; the presented several-km shortening is an estimation and is derived from the preserved offsets within the map (Fig. 2) and the profile (Fig. 10). The thrusts themselves are easily identifiable (Collet & Parejas, 1931) in the field (i.e. by the offset of the Mesozoic strata and basement rock incorporation; see also Figs. 2,10). The evidence for the thrusts is now presented with more clarity in Sect. 4.2. and Figs. 10a,b.

Line 344: was really shown that incorporation of basement slivers in the cover is associated to the 1st deformation phase?

Response: We do agree there is need to better show this wedging-in. We do so by adding Figs. 10a,b to explicitly illustrate the incorporation and the resulting cross-cutting relations.

Line 361: how significant?

Response: At least > 2 km in the JSW in the Rottal section (as can be seen in Figs. 2 & 10). An related statement was added in parenthesis with reference to Fig. 10.

Line 365: repetition of 361

Response: Removed to avoid redundancy.

Line 369: so why should they be called shear zones?

Response: We address this by clarifying the wording and now calling them faults (F1 for the steep faults; "Gadmen" of Berger et al. 2017; and F2 for the oblique to strike slip set; "a-c" joints of Ustazeswksi et al., 2007). We rephrased the last paragraph of Sects. 4.2.1, 4.2.2 and concerning parts in section 5.3.3. We corrected the names in Fig. 9 and added a clarification to the caption of Fig. A2.

Line 380-384: So S1 is at < 330_C, shows dynamic rexx of quartz, but no fabric in the basement, as stated in Line ...?

Response: We do indeed not see any related deformation in the basement, otherwise we would expect to find some fabric formed by dynamic recrystallization. S1 and SZ1 are only found in the sedimentary cover.

Lines 386 – 388: so … under which T conditions did these shear zones develop?

Response: The structures of SZ1 or SZ2 formed under similar conditions, maybe with slightly lower temperatures for SZ2. We stated so previously in Sect. 4.2 and do now so in more clarity in the revised manuscript (see also comments and responses on Lines 183 to 266).

Lines 390-392: An amazing change of scale of interpretation!

Response: We rephrased the sentence to clearly indicate the large-scale linkage to orogenic processes.

Lines 394-395: 3remaining compressional orogenic forces": I think these speculations are not really necessary.

Response: We agree that this discussion goes beyond the scope of this paper, and therefore (and to ensure a concise paper) the half-sentence was removed.

Line 400: "aggravated": aggravating a link? First, it sounds quite dramatic, second it's not the link, but its interpretation that may be "aggravated"

Response: Corrected to "characterized".

Line 404: "is key": structure of the sentence needs to be reconstructed.

Response: The sentence was split into two and the redundant "is key" was deleted.

Line 405: "and discrete":?

Response: Unnecessary words were removed to make the sentence more concise.

Lines 404-406: "while" and "whereas" is too much for the same sentence. Needs to be reformulated.

Response: "whereas" changed to "despite".

Line 406: "bulk of the rock behaved in a brittle manner": do you mean that between the shear zone the rock was also deforming but in a brittle manner? Not clear.

Response: Clarified by specifically labelling the bulk of the crystalline basement rocks as the brittle behaving.

Line 410: "multiphase tectonics": strange term.

Response: Changed to "multiphase deformation".

Lines 411- 412: "the structural imprint … .sets up the stage for erosion": strange statement. I guess the authors wish to say that the steeply oriented displacements created uplift and exhumation by erosion?

Response: This is a misunderstanding. In fact, the steep displacements in combination with the subsequent thrusts provided ideal boundary conditions for preferential erosion to produce the morphological contrast in front of the Aar massif. The sentence was modified accordingly.

References

Berger, A., Wehrens, P., Lanari, P., Zwingmann, H. and Herwegh, M.: Microstructures, mineral chemistry and geochronology of white micas along a retrograde evolution: An example from the Aar massif (Central Alps, Switzerland), Tectonophysics, 721, 179–195, doi:10.1016/j.tecto.2017.09.019, 2017.

Burkhard, M.: Calcite twins, their geometry, appearance and significance as stress-strain markers and indicators of tectonic regime: a review, J. Struct. Geol., 15(3–5), 351–368, doi:10.1016/0191-8141(93)90132-T, 1993.

Burkhard, M.: L'Helvétique de la bordure occidentale du massif de l'Aar (évolution tectonique et métamorphique), Eclogae Geol. Helv., 81(1), 63–114, doi:10.5169/seals-166171, 1988.

Collet, L. and Paréjas, E.: Géologie de la chaîne de la Jungfrau, Beiträge zur Geol. Karte der Schweiz, n.s. 63,1931.

Glotzbach, C., Reinecker, J., Danišík, M., Rahn, M., Frisch, W. and Spiegel, C.: Thermal history of the central Gotthard and Aar massifs, European Alps: Evidence for steady state, long-term exhumation, J. Geophys. Res., 115(F3), F03017, doi:10.1029/2009JF001304, 2010.

Herwegh, M. and Pfiffner, O. A.: Tectono-metamorphic evolution of a nappe stack: A case study of the Swiss Alps, Tectonophysics, 404(1–2), 55–76, doi:10.1016/j.tecto.2005.05.002, 2005.

Herwegh, M., Berger, A., Baumberger, R., Wehrens, P. and Kissling, E.: Large-Scale Crustal-Block-Extrusion During Late Alpine Collision, Sci. Rep., 7(1), 413, doi:10.1038/s41598-017-00440-0, 2017.

Kennedy, L. A. and White, J. C.: Low-temperature recrystallization in calcite: Mechanisms and consequences, Geology, 29(11), 1027, doi:10.1130/0091-7613(2001)029<1027:LTRICM>2.0.CO;2, 2001.

Stipp, M., Stünitz, H., Heilbronner, R. and Schmid, S. M.: Dynamic recrystallization of quartz: correlation between natural and experimental conditions, Geol. Soc. London, Spec. Publ., 200(1), 171–190, doi:10.1144/GSL.SP.2001.200.01.11, 2002.

Ustaszewski, M., Herwegh, M., McClymont, A. F., Pfiffner, O. A., Pickering, R. and Preusser, F.: Unravelling the evolution of an Alpine to post-glacially active fault in the Swiss Alps, J. Struct. Geol., 29(12), 1943–1959, doi:10.1016/j.jsg.2007.09.006, 2007.

Valla, P. G., Rahn, M., Shuster, D. L. and van der Beek, P. A.: Multi-phase late-Neogene exhumation history of the Aar massif, Swiss central Alps, Terra Nov., 28(6), 383–393, doi:10.1111/ter.12231, 2016.

Linking Alpine deformation in the Aar Massif basement and its cover units – the case of the Jungfrau-Eiger Mountains (Central Alps, Switzerland)

David Mair[1], Alessandro Lechmann[1], Marco Herwegh[1], Lukas Nibourel[1], Fritz Schlunegger[1]

[1] Institute of Geological Sciences, University of Bern, Baltzerstrasse 1+3, CH-3012 Bern

Correspondence to: David Mair (david.mair@geo.unibe.ch)

Abstract. The NW rim of the external Aar Massif was exhumed from ~10 km depth to its present position at 4 km elevation above sea level during several Alpine deformation stages. Different models have been proposed for the timing and nature of these stages. Recently proposed exhumation models for the central, internal Aar Massif differ from the ones established in the covering Helvetic sedimentary units. By updating pre-existing maps and collecting structural data, a structural map and tectonic section was reconstructed. Those were interpreted together with micro-structural data and peak metamorphic temperature estimates from collected samples to establish a framework suitable for both basement and cover. Deformation ~~T~~temperatures ~~at deformation~~ ranged ~~d~~ between ~~from~~ 250°C ~~to~~ and 330°C allowing for semi-brittle deformation in the basement rocks, while the calcite dominated ~~sediments~~ sedimentary rocks deform ~~ductile~~ in a ductile manner at these conditions. Although field data allows to distinguish multiple deformation stages before and during the Aar Massifs ~~rise~~exhumation, all related structures formed under similar P, T conditions at the investigated NW rim. In particular w~~W~~e find that the exhumation occurred during 2 stages of shearing in the Aar Massif's basement, which induced in the sedimentary rocks~~s~~ first a phase of folding and then a period of thrusting, accompanied by the formation of a new foliation. ~~We can link this uplift and exhumation history to recently published large-scale block extrusion models.~~

1 Introduction

The Aar Massif is the largest External Crystalline Massif (ECM) in the Alps, made up of exhumed pre-Triassic basement rocks and Mesozoic to Cenozoic sedimentary cover ~~sediments~~ rocks along its N~~W~~E ~~to SE~~ striking frontal margin. In this region, the Eiger, Moeë~~ö~~nch and Jungfrau mountains in the Swiss Alps feature an immense topographic expression along this ~~SE~~ NW-striking rim, with north faces that are characterized by almost 1800 m of ~~vertical~~ difference in elevation ~~offset in their north faces~~. Throughout their stepwise, pyramidal headwalls these mountain ranges expose both the pre-Alpine crystalline substratum and ~~the~~ its ~~at~~ Mesozoic sedimentary cover. ~~rocks of the Aar Massif.~~ These scenic outcrops are thus key to understand ~~ing~~ the Massif's exhumation from ~10 km depth to its present position at 4 km elevation above sea level. Therefore, these mountains have been the focus of a long tradition of structural research, which yielded a general picture of a steeply dipping autochthonous sedimentary cover ~~sediments~~ in front of an up-domed ECM (e.g. ~~i.e.~~ Pfiffner, 2014). Further to the NW are the detached fold-and-thrust nappes of the Upper Helvetics, the ~~, which's~~ Alpine evolution of which is ~~are~~

considered to have been decoupled from the massif's Alpine ~~evolution~~development in an early stage. ~~, an~~T~~d t~~he Helvetic units have experienced a phase of passive up-doming in response to the rise of the Aar Massif after their displacement into a frontal position in the NW during the Oligocene (~~ei.ge~~. Schmid et al., 2004, Hänni ~~&~~and Pfiffner, 2001). The lithostratigraphic and tectonic studies, which resulted in the reconstruction of this scenario, have been conducted over the course of more than 150 years (~~e.gi.e~~. Escher von der Linth, 1839; Baltzer 1880) and have mainly been focused on a few key regions of this ECM. These mainly include: The S and SW sectors of the Aar Massif (i.e. Krayenbuhl ~~&~~and Steck, 2009; Herwegh ~~&~~ and Pfiffner, 2005; Steck, 1984; Steck, 1968), and the area surrounding the Jungfrau and the Moeëonch mountains (i.e. Rohr, 1926; Scabell, 1926; Collet and Paréjas, 1931; Günzler-Seifert and~~&~~ Wyss 1938; Kammer, 1989 and references therein). Farther to the NW ~~in the region of the Bernese Oberland~~, the neighboring Mesozoic sedimentary rocks~~s~~ have been studied ~~later~~ in detail, an overview is found in ~~(i.e.~~ Hänni ~~&~~ and Pfiffner~~,~~ (2001)~~.;~~ Menkveld~~,~~ (1995~~;~~), Pfiffner~~,~~ (1993) and references therein~~)~~.

The best-studied region of the Aar Massif is the Haslital that~~,~~ ~~which~~ stretches from Innertkirchen up to the Grimsel Pass (Abrecht, 1994 and references therein) and which exposes the crystalline rocks of what has been referred to as the Central Aar Massif. ~~A swath of petrological and chronological data~~New $^{40}Ar/^{39}Ar$ and Rb/Sr ages for syn-kinematically formed fault zone micas (i.e. Challandes et al., 2008; Rolland et al., 2009; Schaltegger et al.,~~;~~ 2003) together with structural observations (i.e. Wehrens et al., 2017, Wehrens et al., 2016~~,~~) and K-Ar ages for fault zone micas (Berger et al., 2017a) advanced ~~our~~ the understanding on the geodynamic evolution of the Aar Massif. ~~This culminated in a new model for the exhumation of the Aar Massif (Herwegh et al. 2017)~~A compilation of peak metamorphic temperature and deformation age data as well as calcite-dolomite geothermometry, culminated in a new model for the exhumation of this unit (Herwegh et al. 2017), and in a new regional-scale geological map (Berger et al., 2017b). Nevertheless, details about how the tectonic deformation affected the crystalline basement and the sedimentary cover rocks of Aar Massif, and if and how this deformation propagated into the sheared-off Helvetic nappe system in front of the Massif have not been explored in detail for the Jungfrau-Moeëonch area. This is mainly due to the complexity of the geologic architecture and the inaccessibility of the area that have thwarted a precise reconstruction of the history ~~and the amount of shortening~~ of the frontal part of this Massif. It is the scope of this paper to link the tectonic history of these uplifted basement blocks to the structures in the cover ~~and to fill this knowledge gap~~.

Here, we reconstruct the relative chronology of the frontal part of the Aar Massif in 3D. We focus on the central part presently exposed in the Central Swiss Alps, where this contact is exposed c. 12km along the strike of the basement cover ~~boundary~~interface. We proceed through (i) establishing a synthesized lithostratigraphic framework for the region, (ii) collecting new structural data and samples on the surface ~~in the field~~ and along the "Jungfraubahnen" railway tunnel that crosses the mountain range, and through (iii) modeling the tectonic architecture with GIS and Midland Valley's (new Petex) Move™ software package. We differentiate the sedimentary cover ~~sediments~~ rocks based on stratigraphic criteria, which in turn allows us to reconstruct the geometry of the exposed units. ~~In addition, s~~Structural data ~~analysis~~ enables us to unravel

their relative deformation ~~history~~, while Raman Spectroscopy on Carbonaceous Material (RSCM) yields estimates on peak metamorphic temperature. Our synthesis of existing data together with new observations finally allows us to link the fabric of the sedimentary cover ~~sediments~~ rocks with the underlying basement units' evolution for one of the Alps' most famous scenery. This results in a new picture of how the differences in rheology have controlled both mesoscale deformation structures and micro-scale deformation style as well as the bedrock fabric of the crystalline basement and the overlying sedimentary cover lithologies.

2 Geological setting

2.1 Tectonic architecture

The Aar Massif is ~~the largest External Central Massif (ECM) in the Alps and is~~ made up of polymetamorphic pre-Variscan gneisses with intruded post-Variscan granitioids (Labhart, 1977; Abrecht, 1994). The most external polycyclic gneiss unit is exposed along the Aar Massif's northwestern rim, referred to as the Innertkirchen-Lauterbrunnen zone (ILZ; Berger et al., 2017~~a~~b; Abrecht, 1994; Fig. 2). Farther to the SE, the Erstfeld Zone exposes gneiss units (EZ; Abrecht, 1994) and occurs in a hanging wall position to the ILZ (Berger et al., 2017b; Fig. 2) with ~~sediments~~ sedimentary rocks squeezed in-between these two gneiss units. This tectonic sliver made up of sedimentary and crystalline rocks is referred to as Jungfrau-Sediment-Wedge (JSW). Both units share a concordant overall SW-NE strike direction of structures such as lithological boundaries and foliations (Oberhänsli et al., 1988). These pre-Variscan basement units experienced multiple periods of deformation and metamorphic overprint, which occurred during the Proterozoic, Ordovician, Variscan, the Late Cretaceous and the Cenozoic (Steck, 1968; Labhart, 1977; Schaltegger, 1993; Schaltegger et al., 2003). In our study area (Fig. 1) and farther to the west, the EZ is separated from the ILZ by this wedge of Mesozoic sediment~~s~~ary rocks (Krayenbuhl and~~&~~ Steck, 2009; Herwegh and~~&~~ Pfiffner, 2005; Steck, 1968). Additional autochthonous Mesozoic sedimentary cover ~~sediments~~ rocks are present at the NW rim of the Aar Massif (Kammer, 1989), where they form an own, detached and transported nappe system (Doldenhorn nappe; Herwegh and~~&~~ Pfiffner, 2005; Burkhardt, 1988).

The sediment wedges and the Mesozoic cover were only affected by ~~Alpine~~ deformation and metamorphism of Alpine age. In the study area, the Alpine metamorphic overprint occurred under lower greenschist metamorphic conditions (Frey and~~&~~ Mählmann, 1999; Niggli and~~&~~ Niggli, 1965), which is recorded by the occurrence of distinct metamorphic index minerals and illite crystallinity~~)~~. The peak metamorphic temperatures increased towards the SE, where conditions of ~450°C and 6.5 kbar have been reconstructed for the Cental Aar Massif granitoid shear zones (Challandes et al., 2008) at a time around 20 Ma (Wehrens et al., 2017; Herwegh et al., 2017).

2.2 Alpine structural evolution

The structural imprint of this ECM has been related to various deformation stages by multiple authors (Table 1), often depending on ~~the~~ site-specific conditions. This resulted in the generally accepted notion that during the late Eocene, the Helvetic sedimentary nappes were detached from their crystalline substratum situated farther to the SW (Pfiffner, 2014; Herwegh ~~&~~and Pfiffner, 2005; Burkhard, 1988). Thi~~s~~ese ~~mechanisms~~ process appears not ~~to~~ be recorded by the structural fabric in the Aar Massif's basement (Wehrens et al., 2017; Berger et al., 2017a). This has been used as ~~argument in geodynamic work~~ to disconnect the evolution of the basement rocks from that of the Helvetic cover ~~sediments~~ nappes (e.g. Pfiffner, 201~~5~~4). An early ~~deformation fabric assigned to~~phase of NW directed Helvetic thrusting, the "Plaine Morte" phase of deformation, is recorded in the western Central Helvetic units only (Burkhard, 1988; Pfiffner, 2014). The subsequent Oligocene phases of deformation, which were referred to as the "Prabé" phase in the west and "Calanda" phase (Milnes and Pfiffner, 1977) in the east of the Helvetic nappes (Burkhard, 1988; Pfiffner, 2014), were associated with the main phase of top to NW dominated thrusting within the Helvetic units, and they are recorded by a penetrative foliation. ~~dominated thrusting within the Helvetic units and are recorded by a penetrative foliation.~~ Further shortening led to the formation of the Doldenhorn nappe (former Infrahelvetic and ~~new~~ now Lower Helvetic), when a former half graben basin was inverted and incorporated into the Alpine edifice. This phase of deformation, which has been referred to as the "Kiental" phase (Herwegh and~~&~~ Pfiffner, 2005; Burkhard, 1988), produced a large-scale recumbent fold (Doldenhorn fold sensu strict~~u~~)o and likewise induced a period of passive folding in the overlying Helvetic nappes. By the end of this phase, at around 20 Ma, the Helvetic nappes (Upper Helvetics) existed in positions ~~were placed~~ in front and on top of the future Aar Massif with an inverted stratigraphic ~~an inverse~~ succession, where the Autochthon and the Doldenhorn nappe (Lower Helvetic) were situated below these nappes (Herwegh and~~&~~ Pfiffner, 2005).

The exhumation history of the crystalline basement rocks of the Aar Massif, generalized as "Grindelwald" phase (~~Güntzler-Seifert, 1945;~~ Burkhard, 1988), records the following multistage late-Alpine deformation sequence: (i) First, steeply south dipping reverse and normal faults developed a set of pervasive shear zones during the "Handegg" ~~phase of~~ deformation (Wehrens et al., 2016; Wehrens et al., 2017), with a progressively increasing ~~differential~~ uplift component towards the south (Herwegh et al., 2017). ~~Subsequently~~This was followed by~~,~~ a phase of strain partitioning ~~occurred simultaneously~~ with (ii) dextral strike slip to oblique slip shearing along NW-SE and WNW-WSE trending faults ("Oberaar" phase) in the south and (iii) NW directed thrusting ("Pfaffenchopf" phase) along moderately southeast dipping fault planes (Labhart, 1966; Wehrens et al., 2016; Wehrens et al., 2017; Herwegh et al., 2017; Berger et al., 2017a). During this latter deformation phase~~, the uplift passively rotated~~ the former main thrust faults and foliation of the Helvetic and Doldenhorn nappes were passively rotated (Burkhard, 1988). This ~~supposedly~~ was inferred to have resulted in ~~lead to~~ the present, almost vertical orientation of the main Helvetic thrust in front of the Eiger (Pfiffner, 2014). The latest deformation stage ("Gadmen" phase) is recorded by a steep, NE-SW trending northern block with brittle deformation structures, ~~(~~which are characterized by mostly steep, cataclasitic reverse and normal faults with cm~~-~~-sized offset~~s~~; (Labhart, 1966; Berger et al., 2017a).

3 Methods and data

A regional structural map was produced (Fig. 2) with the aid of remote sensing techniques. This map was reconstructed by compiling geological and structural information from previous maps (for a review of the data sets used see Appendix A). These were verified and updated by own mapping in the field. Special focus was directed towards the mapping of stratigraphic contacts in the sedimentary cover ~~sediments~~ rocks and of shear zones in the basement, both on outcrop and regional scales. ~~Field mapping was done using the 1:25'000 Topographic Map of Switzerland as basis, which was enlarged to a working scale of 1:10'000.~~ We ~~additionally~~ employed high resolution orthophotos (raster resolution 0.25 x 0.25 m; provided by swisstopo) and a high-resolution digital elevation model (swiss ALTI3D, version 2013 provided by swisstopo) as bas~~i~~es for mapping. Structural data (orientation of bedding, lithological contacts, foliation, lineation and faults) were collected with a traditional geological compass and a handheld GPS. The structural dataset was expanded by producing a ~~lineation~~ lineament map, i.e. fault induced morphological incisions, thereby following the workflow of Baumberger (2015), Baumberger et al. (in press) and Schneeberger et al. (2017), which in turn is based on Rahiman ~~&~~and Pettinga (2008). We only mapped ~~only~~ lineaments that were visible both on the DEM and aerial images, and that were readily identifiable in the field. Lineaments that were observed on remotely sensed datasets ~~only~~ are indicated as "inferred". Orientations thereof were obtained by plane fitting through moment of inertia analysis of georeferenced point data using the method of Fernández (2005). In addition, we completed the geologic map through collection of geologic information in the "Jungfraubahnen" railway tunnel. The tunnel runs oblique to parallel to the striking direction of the main structural elements between ~3000 m elevation in the E and ~3400 m in the west (Fig. 2).

The map was combined with microstructural observations on thin sections. Thin sections were cut parallel to stretching lineation and normal to foliation planes, thus allowing shear sense directions to be identified. In addition, we used thin section observations to qualitatively estimate the temperature ~~conditions~~ during peak metamorphic conditions and during periods of dynamic recrystallization of quartz and calcite aggregates.

Raman spectroscopy on carbonaceous material (RSCM) was used for peak temperature estimations recorded by the Mesozoic ~~sediments~~sedimentary rocks. The RSCM technique quantifies the degree of graphitization in meta-sediments, which is a reliable indicator of peak metamorphic temperature (Beyssac et al., 2002). RSCM measurements were performed with a Jobin Yvon LabRAM-HR800 instrument at the Institute for Geological Sciences at the University of Bern. An Nd-YAG continuous-wave laser (20 mW beam spot of 1 µm diameter and wavelength of 532.12 nm) focused through an Olympus BX41 100x confocal microscope was used. The acquisition of the Raman spectra was monitored with the Labspec 4.14 software of Jobin Yvon. Curve fitting (for histograms see Appendix B) and temperature estimation followed strictly the procedure described in Lünsdorf et al. (2014), Lünsdorf and Lünsdorf (2016) and Lünsdorf et al. (2017). The absolute temperature calibration-based error is in the order of ±40°C, however, relative temperature differences can be resolved down to ±15°C (Lünsdorf et al., 2017).

4 Results and interpretation

We present an inventory of structural rock fabrics (both on outcrop and microscale) of the studied area. These fabrics developed during Alpine deformation and are different for the sedimentary cover ~~sediments~~ rocks and for the basement ~~rocks~~lithologies.

4.1 Host rock characteristics

4.1.1 Polymetamorphic Aar Massif basement rocks (ILZ ~~&~~and EZ)

The basement~~s~~ rocks of the ILZ and the EZ consist of~~are present as~~ plagioclase, alkali feldspar and quartz dominated gneisses, which are occasionally enriched in micas (mainly biotite and white micas) and chlorite minerals (Fig. 3, second row). In the study area, the texture ranges from typical coarse-grained~~pical~~ granoblastic (the largest grain size of feldspars is < 2 cm) to ~~granodioritic~~ fine-grained granoblastic (grain sizes of <<1mm) for the matrix zones of the migmatites (Rutishauser, 1973). Usually the feldspars (both alkali feldspar and plagioclase), together with biotite, form large grains with interstitial quartz. This texture is only partially preserved, due to a later greenschist facies overprint.

This overprint is recorded by chlorite replacing biotite and quartz, sericitization of feldspar grains, as well as by the growth of interstitial white mica (~~see also~~ Berger et al., 2017b). The overprint, however, did not completely erase the original high temperature fabric ~~completely~~, instead it often forms core-rim structures around altered feldspar grains (Fig. 3: second row). Quartz aggregates still preserve the original texture. No new biotite growth occurred and no preferred orientation, ~~(~~neither for quartz nor micas,~~)~~ on the microscale is found. This aligns well with the lack of evidence~~d~~ for an Alpine foliation on the outcrop scale in some basement rock outcrops outside discrete shear zones.

4.1.2 Mesozoic sedimentary cover ~~sediments~~rocks

The Mesozoic ~~cover sediments~~strata form an originally up to 500m-thick succession of limestones, mudstones and sandstones (Fig. 4; for detailed discussion see Appendix A). The stratigraphic suite can be synthesized into eight larger units (Fig. 4 ~~&~~and Table 2). This allows to distinguish the main stratigraphic horizons, and to group units with similar mechanical strengths (see also Pfiffner, 1993; Sala et al., 2014). These units comprise: the Triassic (Mels~~-~~, Quarten~~-~~ and Roeöti Fms.), the Mid Jurassic (Bommerstein~~-~~ and Reischiben Fms.; "Dogger"), the Upper Jurassic A (Schilt Fm.) and B (Quinten Fm.), the Lower Cretaceous A (OeÖhrli Fm.) and B ("Helvetic Kieselkalk" and Betlis Fm.), the "Siderolithic" and the Tertiary units.

There are several main characteristics needed to understand the structural fabrics within the individual sedimentary units. The basal Triassic, above the weathered basement-cover-contact, is formed by crystallized cellular dolomites and shales (Appendix Fig. A1). Despite varying thicknesses (5m- 50m) and ~~stratigraphic~~ lithologic ~~contents~~characteristics, it is present throughout the entire study area. The 250m to 300m-thick suite of Upper-Jurassic limestones, and the overlying up to 150m-

thick succession of Lower Cretaceous limestones form the bulk of the strata and are constant in thickness throughout the studied area. The only difference between the facial domains (Fig. 4; aside from a thicker Lower and Mid Jurassic strata) is the presence of a Cretaceous B unit (in the northern flanks of Jungfrau and Eiger), which consists of layered cherts with limestone interbeds. Note that these features allow its identification as continuation of the Doldenhorn nappe farther to the west.

4.2 Deformation structures

The studied mountain chain is dissected by numerous high strain zones with variable orientations, which occur both in the basement and in the sedimentary cover~~. Note that we refer to as shear zones for fabrics, which formed through ductile or semi-ductile deformation mechanisms. Only for brittle-dominated structures (cataclasite and gauge-dominated) we apply the term fault.~~.

4.2.1 Basement strain localization

Locally, a weakly ~~pronounced~~developed, pre-Alpine foliation can be found. If preserved, it is usually cut or overprinted by Alpine ~~exhumation related~~ structures. These latter structures generally occur as discrete sub-mm- to meter-thick shear zones in the field (Fig. 5a). ~~-~~They are present either as a set of generally steep or as a set of intermediate S dipping semi-brittle to brittle faults forming on former shear zones ~~shear zones~~ (Fig. 5). These steep faults on~~-~~ reactivated~~ing~~ shear zones, which we define as SZ2 (Figs. 3 and~~&~~ 6; Note that SZ1 shear zones were only found in the ~~sediments~~sedimentary rocks), exhibit normal and reverse kinematics ~~faulting behavior~~ with dominantly top to the NW shear senses, as is indicated by the offset of older structures (Figs. 5b,c) and by dip-slip stretching lineation (Fig. 6a). ~~However, s~~ Several individual faults show evidence for reverse movements as documented by displacements of isolated dm-sized blocks. Typical Riedel shears are present, highlighting the conjugate semi-brittle nature of the shear zones. The spacing between them decreases towards the NW and close to the JSW. In the Rottal (RT), the mean orientation of these structures is 315/84 (dip azimuth/dip) with indications for up-movements of the southern blocks~~with south-block-up movement~~. In the Trugberg (TB) zone the average dip azimuth is 180/52 (inferred from remote sensing). Note that owing to younger deformation overprint, the original orientation might have been different than at present.

~~The~~ An intermediat~~ly~~e steep set of shear zones (SZ3; Fig. 6) cuts and offsets the SZ2~~.~~ structures. The spacing of the shear zones is in the order of tens of meters ~~spacing is~~ and therefore much wider compared to the centimeter to meter ~~and~~scale of SZ2. In addition, the SZ3 ~~the~~ deformation ~~occurred~~ is more localized (especially within the JSW; Fig. 5). The orientation of the SZ3 suites also changes from moderately steep SE dipping to NW dipping in the NW (TB: 157/22 vs. RT: 351/27) with NW plunging stretching lineations (RT: 322/21). The shear sense of SZ3 is characterized by top to NW thrusting (Figs. 6a, 8).

Despite the differences in orientation and kinematics, the microfabrics of both SZ2 and SZ3 samples show no difference in terms of deformation microstructures and mineral assemblages. Grains of the original pre-Alpine granoblastic fabric are either replaced by new grains of much smaller size (i.e. chlorite, white mica, epidote; Fig. 3; 3rd row), which are well-foliated, or they experienced mechanical grain size reduction down to a few micrometers. Th~~o~~ese small-grained minerals are often concentrated in micrometer to centimeter~~-~~-thick polymineralic bands. They form S-C fabrics and shear bands (Fig. 3). However, feldspar and quartz minerals are still present as porphyroclasts despite evidence for incipient dynamic bulging recrystallization for quartz (see also Bambauer et al., 2009). Notable is the higher phyllosilicate content in shear zone rocks compared to the host rock composition.

A youngest set of (i) SE-NW striking steep faults (F1) ~~(i) NW-SE running, sub-vertical fault planes ("ac joints" of Ustazeswksi et al., 2007)~~ and (ii) NW-SE oriented, sub-vertical fault planes (F2) ~~(ii) SE-NW striking steep faults (Fig. 6c and Fig. 9b) that~~ cut all older structures (Figs. 6c, 9b) and are characterized by brittle deformation forming cataclasites, fault breccias and gauges (Appendix Fig. A2). Both fault sets cross-cut all other structures and are best detected in the subsurface (along the "Jungfraubahnen" tunnel; Fig. 2), due to their susceptibility to weathering. Set F1 mainly features mm- to cm-wide fault zones along a set of open joints. However, the offset of these faults is in the order of a few centimeters to meters and is thus not resolvable at the scale of Figures 2 and 10. Set ~~(i)~~F2 shows oblique to strike-slip kinematics (Fig. S3) in cm to m wide cataclasitic shear zones, often with fault gauges at the core. ~~Set (ii) mainly features mm-to-cm-wide shear zones along a set of open joints. However, the offset of these faults is in the order of a few centimeters to meters and is thus not resolvable in Figures 2 and 10.~~

4.2.2 Deformation in the sedimentary cover ~~sediments~~rocks

The ~~cover sediments~~sedimentary rocks show strong evidence for ductile deformation and brittle deformation, both on outcrop scale and in thin sections. ~~Mapping reveals that the deformation fabric is dependent on the rheology of the hosting rocks.~~ The calcite-dominated limestones exhibit a strong ductile overprint, expressed by complete dynamic recrystallization of the original fabric with grains that are smaller than 25 µm (Fig. 8). They show a well-developed foliation (S1) parallel to the bedding in most of the study area, which formed through abundant calcite dissolution and dynamic recrystallization. This first mylonitic ~~foliation~~fabric (S1) shows a foliation spacing ~~-~~ranging from several cm in the lower RT (Rottal) section to <<1mm in the Moeënch~~ss~~joch (MJ). Typically, it overprints the bedding completely (Fig. 7). Notably the Triassic dolomite (Roeëti Fm.) was not deformed in a ductile, but rather in a brittle or semi-brittle manner. This is expressed in abundant bookshelf structures and "domino-like" boudins (Fig. 7c) affected by more than one deformation phase ~~(Fig. 7c)~~. These rigid lenses are stretched out along shear planes or form kink folds near the basement cover interface. The same applies to mid Jurassic iron-rich sandstones and Cenozoic iron-rich sandstones or iron-carbonate nodules ("Siderolithic"). This ~~led~~ deformation style leads to macroscopic (and microscopic)-scale boudins (Figs. 7 ~~&~~and 8), thereby making these units ideal stratigraphic markers to identify shear zones and stratigraphic polarity (Fig. 2).

In the NW flank of the Jungfrau-Eiger mountains, the Mesozoic ~~sediments~~ strata ~~occur~~are segmented in distinct stacks, separated by arrays of discrete shear zones (SZ1) of < 1 m to up to 5 m widths that are generally aligned parallel to the S1 foliation where the layer spacing decreases towards the shear zones ~~that formed during the formation of S1~~. These shear zones acted as thrusts with a general top to NW displacement direction. They were accompanied by the circulation of metamorphic fluids, as testified by abundant iron-rich, micrometer-thick layers of precipitated minerals. Growth of white mica and chlorite minerals within the pressure shadows is frequently observed, mainly in non-calcite dominated lithologies. These thrusts contain slivers of ILZ basement rocks ~~in~~ of the footwall, which are now incorporated in the sedimentary stacks (~~ei~~.ge. in the Rottal area, Figs. 2,10).

Subsequent to the SZ1 thrusting, anti-clockwise rotation of the initial structures (bedding and S1, in section view, looking E) was accomplished by local folding near the basement cover contact. The folding produced SE dipping and SW/W to NE/E striking axial planes, which locally form an axial plane foliation (S2). This deformation affected the sedimentary rocks in an asymmetric way, where folding became more intense towards the SE, culminating in a dm-spaced axial plane foliation (S2) in the JSW (Fig. 7e). ~~is documented by rotated sigma clasts in the shear zones (and the mineralized veins within them; Fig. 7).~~ As a result, the present-day orientation of S1 varies form SE dipping (118/35 for region EN, 118/36 for region EW; see Figs. 2 and 9 for locality) in the lower para-autochthonous slice, to the NW dipping (312/22 for GG; 297/36 for EM; Fig. 9). ~~The original orientation is not preserved. This deformation stage affected sediments in an asymmetric way, and the folding is intensified towards the SE of the studied area~~. ~~Consequently, these structures culminate in a weak dm-spaced axial plane foliation (S2) in the JSW.~~

Subsequent NW-directed shearing led to a further thinning of favorably SE dipping or flat lying aligned thrust-planes of S1 fabrics in the now flat lying limbs of the stacked imbricates (Fig. 1~~01b~~). The new foliation (S3) formed often parallel (or only cutting under low angles) to the pre-existing mylonitic foliation (~~ei~~.ge. Figs. 7a,d). In cases where S1 structures dip ~~in an unfavorably~~ steeply to the NW ~~orientation~~ (e.g.~~as it is the case~~ in RT region or at the location of Fig. 7b~~5~~), the local new foliation (S3) developed still under the same orientation, cutting the older foliation (S1) at high angles (Figs. 7b, 10). This foliation features evidence for slip where S1 fabrics are cut. Dip azimuth alters between gently SE dipping, flat lying and NW dipping, with a dominant top to NW sense of shear~~thrust~~, indicated by stretching lineation data derived from abundant calcite slickenside striations on S3 slip planes. This shearing occurred still under ductile conditions for calcite.~~,~~ ~~h~~However non-limestone dominated lithologies, which includes ~~(including incorporated~~ basement slivers~~)~~, exhibit shear localization merely by mechanical grain size reduction of minerals to a few microns. They form a microcrystalline cataclasit~~e~~ic fabric consisting mainly of quartz, white mica, chlorite, epidote and feldspar.

The latest ~~deformation stage produced~~ a set of brittle sub-vertical faults striking NW-SE (F1) and steep SW~~-~~ ~~and~~ NE striking oblique oriented brittle fault~~s zones~~ with evidence for strike slip and reverse/normal fault behavior (FSZ24) ~~and brittle sub-vertical faults striking NW-SE~~. Both are found within ~~sediments~~ basement and cover rocks of all levels ~~alike~~ (documented by fault breccia and mineralized veins crosscutting an older set; Appendix figure A2). These overprint all ~~younger~~ other

structures. Due to the brittle nature and connection to the surface they are often water saturated and highly susceptible to weathering. Despite cutting across all units, offsets (if even present) are limited to a few centimeters only and are thus not visible on map scale.

4.3 Peak metamorphic temperature

Raman spectroscopy applied to carbonaceous material (RSCM) was used on 8 selected samples representing the different tectonic levels in the studied area to constrain peak Alpine metamorphic temperatures for the sedimentary cover ~~sediments~~ (Table 3). Results yield the lowest temperatures for the presently lowest elevation sample (LAU-02: 283±14°C at 838 m a.s.l. for the Upper Jurassic limestone) and samples from the Eiger north flank (EN-01: 283±12°C at 2388 m a.s.l.). Slightly higher peak temperatures are obtained for samples collected at the Eiger summit (EG-17-01: 292±10°C at 3970 m a.s.l.). Highest temperatures are found in the JSW samples (MJ-03 and MJ-06: 308±14°C and 317±11°C respectively). The data indicate a trend to slightly higher temperatures towards the more internal units in the SE. ~~Assuming~~ We employ a constant average geothermal gradient of ~~25~~27°C km^{-1} (Schlunegger and Willet, 1999; Glotzbach et al. (2010); Valla et al., 2016), falling in the global range for the upper continental crust ~~(Pollack & Chapman, 1977)~~ for the past (Pollack and Chapman, 1977)~~,~~. Thus, we are able to reconstruct the approximate minimum sample depth at peak metamorphic conditions. This allows us to identify the vertical position of the corresponding units relative to each other. The overall temperature range of 283°C to 317°C indicates a sample depth between 10.5~~1~~ and 13~~2~~ km, or even shallower, at peak temperature conditions. This further constrains the peak temperature for the crystalline substratum of these ~~sediments~~ sedimentary rocks to <330°C.

4.4 Imbricate geometry in the sediment~~s~~ary cover

Stratigraphic markers (see Sect. 4.1.2) are used to delineate geometrical ~~bodies~~ units separated by thrusts of different generations (see Sect. 4.2.2). From ~~the~~ NW to ~~the~~ SE (and present-day bottom to top) we find the ILZ and its sedimentary cover still in its original position. This is superimposed by two c. 500 thick imbricate stacks ~~of c. 500m thickness~~, with normal stratigraphic succession within each stack (often referred to as "para-~~authochthonous~~autochthonous", Fig. 11~~0~~). On top of these, we additionally find a >1000 m-thick pile of Cretaceous and Jurassic limestones, which was often referred to as the core of a syncline (Krayenbuhl ~~&~~and Steck, 2009). These units are deformed as an ensemble during stage 2 and stage 3 phase of deformation as described in Sect. 4.2.2 (see Fig. 10~~1~~). The subdivision of this sedimentary stack is internally consistent along strike within the study area. Lateral differences in structural style, which occurred in response to the last 2 deformation stages, are expressed by less shortening along the JSW (as shown in map view~~,~~; see Fig. 2) ~~–~~while more basement slabs were detached and thrusted at a lower level. The ensemble of this deformation pattern resulted in a locally steeper (almost vertical) orientation of the basement cover contact. This is mainly due to the large differential block uplift in the basement (SZ2) that passively steepened the sedimentary cover in the SE. ~~.~~

5 Discussion

The ~~cover sediment~~sedimentary cover reveals a set of distinct deformation fabrics that formed during a 3-stage evolution. We derive these stages from aforementioned field data and geometrical relationships. By disentangling the fabrics related to each stage, we can link these in a regional geodynamic context.

5.1 Pre-Alpine inheritance

An important role falls to Paleozoic and older structures that are inherited in the basement (i.e. the polymetamorphic basement called "Altkristallin" in the German literature; Steck, 1968). Since the ILZ and EZ were originally sedimentary protoliths (Rutishauser, 1973; Rutishauser, 19734; Schaltegger, 1993) they feature a heterogeneous architecture (i.e. Abrecht, 1994). Large scale partial melting produced the original host rock fabric (Sect. 4.1.1). Radiometric dating yielded Ordovician ages for the high temperature metamorphic overprint of the EZ~~rstfeld zone~~ (456±2 Ma) and the ILZ~~nnertkirchner Lauterbrunnen migmatites~~ migmatites (452±5 Ma; Schaltegger, 1993) ~~for this high temperature metamorphic overprint~~. Thus, any evidence of a previous geological history was erased, but the metasomatic overprint preserved to some extent the original heterogenous lithological character (Berger et al., 2017~~ab~~, Abrecht, 1994). Subsequent tectonic events already aligned structures, i.e. lithological boundaries and foliation (Schaltegger et al., 2003), along a SW-NE direction~~, i.e. lithological boundaries and foliation (Schaltegger et al., 2003)~~. The wedging-in of Permian volcanoclastic sediments (Berger et al., 2017b), which was associated with folding, suggests that the basement internal nappe emplacement occurred ~~already~~ during the Carboniferous (Oberhänsli et al., 1988). The emplacement of several late to post-Variscan granitic intrusions completed the pre-Mesozoic evolution of the pre-Alpine basement gneisses and presumably lead to the greenschist facies overprint in the host rocks. The resulting heterogeneities were intermediate to steep S to SE dipping fabrics (Berger et al., 2017~~ab~~), which already formed before the initiation of the Alpine orogenic cycle and therefore represent important mechanical anisotropies for the ~~succeeding~~ Alpine tectonic evolution (Herwegh et al., 2017).

5.2 Stratigraphic priming

Some of the steep SE orientated pre-Alpine heterogeneities were reactivated during the Mesozoic as normal faults within the Helvetic shelf of the Tethys Ocean (e~~i~~.ge. Hänni ~~&~~and Pfiffner, 2001). Strikingly, in the study area, the JSW ~~sedimentary wedge~~ (that should later act as a major thrust) is located at the pre-Alpine boundary between the ILZ and EZ. The ~~favorable~~ SE dipping orientation most likely resulted in the re-activation of these contacts as Jurassic normal faults, causing the stratigraphic NW-SE asymmetry in the Mid-Jurassic (Herwegh and Pfiffner, 2005; Krayenbuhl ~~&~~and Steck, 2009). This allows us to account for the evolution across the former Helvetic shelf. Two important stratigraphic observations can be made in the Mesozoic of the Jungfrau tectonic sliver and associated shear zones: (i) The Triassic sequence is eroded to a deeper level towards paleo-~~-~~SE, owed to the asymmetric Liassic erosion ("Alemannic land": Pfiffner, 2014; Rohr, 1926) and (ii) the subsequent sedimentation in the Middle Jurassic is governed by normal faulting, resulting in thicker sediment

successions at deeper water conditions to the paleo-SEW. Apart from these differences (and the difference in the Lower Cretaceous) the post-rift sedimentary cover ~~sediments are~~is rather similar in thickness and facies throughout the ~~studied~~ study area.

Generally, the autochthonous cover of the Aar Massif comprises a Mesozoic stratum resembling the northwestern-most facies of the Central Helvetic domain in the Lauterbrunnen valley (Bruderer, 1924; Masson et al., 1980; Herb, 1983). On a larger scale, our stratigraphic model aligns well with recent findings, ~~e.g.~~. for the Triassic (Gisler et al., 2007) and for the revised Tertiary stratigraphy of the Helvetic realm (Menkveld-Gfeller et al., 2016). This stratigraphic model (see Fig. 4 and T~~t~~able 2) allows us to bracket ~~unit~~ the thicknesses. We are aware of the partly large uncertainties on these values (sometimes up to 100%), yet it is still useful for ~~omitting~~ avoiding the reconstruction of unrealistic geometries.

5.3 Structural imprint of the Alpine evolution

5.3.1 Early stage deformation under highest Alpine temperature conditions

Alpine ~~P~~peak metamorphic conditions are constrained by the RSCM estimates to low temperature (sub-greenschist facies) conditions for the sedimentary cover ~~sediments~~ and the immediate crystalline substratum. An upper temperature limit ~~for the calcite thermometry~~ is provided by the ~~graphite~~ RSCM data from the most internal part of the JSW (Table 3) at ~320°C. Since the bulk of the Mesozoic strata consists of limestones (Fig. 2) the temperature range for the deformation has a lower constraint of ~~200~~150-250°C, which governs the onset of the ductile deformation of calcite (Herwegh et al., 2005, Kennedy and White 2001, Burkhard 199~~3~~0). These conditions align well with reported regional Alpine metamorphic gradients (~~e.g.~~ Herwegh et. al., 2017; Niggli ~~&~~and Niggli, 1965). Only at temperatures as high as ~300°C or above, onset of ductile deformation in quartz occurs, as can be inferred from the occurrence of dynamic recrystallization in form of bulging recrystallization (e.g., Stipp et al., 2002; Bambauer et al., 2009; Härtel and Herwegh, 2014). However, our quartz-rich basement rocks were mainly deformed in a semi-brittle manner (see. Sect. 4.2.1) as q~~Q~~uartz and f~~F~~eldspar are ~~in general~~mostly mechanically reduced in grain size within discrete shear zones (Fig. 3; last row). The mylonitic character is primarily owed to ductile behavior of micas, chlorites and the fine-grained polymineralic gauges (~~similar to findings reported by~~ Wehrens et al., 2016; and Wehrens et al., 2017). ~~We see the onset of dynamic recrystallization in quartz through evidence for bulging in some samples. Thus, we must place the development of all shear zones in the basement close to or shortly after peak metamorphic conditions.~~

Contrariwise, the calcite limestone-dominated ~~cover~~ sedimentary rocks ~~sediments~~ were completely recrystallized, along with the growth of new micas in pe~~l~~litic rocks, leading to a pervasive, bedding-parallel foliation (S1). We find thrusts (SZ1) that synchronously utilized ~~rheological~~ weak layers of the Triassic as detachment horizons and Tertiary shales and sandstones as roof thrusts. In case of the Triassic, the cellular dolomites, evaporites and shales (Fig 4) represent mechanically weak lithologies, where strain can be easily localized upon thrusting (Pfiffner, 1993). Along these thrusts the sedimentary cover ~~sediments were~~was detached from their substratum and formed an imbricate stack (see Sect. 4.4, Fig. 1~~1~~2a). Initially, this

occurred by reactivation of steep SE dipping Jurassic normal faults as reverse thrusts, which was a common mechanism for the inversion of the Helvetic shelf during the formation of the Alpine accretion wedge (Krayenbuhl ~~&~~and Steck, 2009; Hänni ~~&~~and Pfiffner, 2001). These thrusts incorporated decameter~~-~~-sized slivers of basement rocks at the base of sediment stacks by the means of footwall shortcut thrusts (McClay, 1992). The shortening accumulated along each of the imbricate thrusts amounted to several kilometers (Fig 10).

This process most likely occurred during a final stage of the detachment of the Helvetic nappes farther to the SE and thus during the late Kiental phase of deformation (Burkhard, 1988; Herwegh ~~&~~and Pfiffner, 2005; Pfiffner, 2014). This scenario clearly contradicts the interpretation of Krayenbuhl ~~&~~and Steck (2007) who interpreted these structures as basement folds, since (i) we do not find signs for ductile folding in the basement rock, but rather the incorporation of large slices of basement rocks in the cover ~~sediments~~; and (ii) these ~~sediments~~ sedimentary rocks are usually found in (thinned-out though) stacks within a normal stratigraphic succession. At the end of this deformation stage the cover sedimentary units were imbricated and stacked upon each other.

5.3.2 Exhumation structures

The early deformation phase did not leave a pervasive imprint in the basement rocks. However, a local basement-associated deformation is manifested by the incorporation of the early basement slivers in the sediment imbricate stack (see black arrows in Fig. 12~~1~~a). This situation changed drastically during the next deformation stage. Here, the steep to sub-vertical SW-NE striking shear zones in the basement rocks developed (SZ2). They generally exhibit a reverse fault character with upward movement of the southern block (Figs. 3, 11b). Such structures can be seen through the whole Aar Massif (Baumberger et al., in press), and express the vertical extrusion of mid-crustal rocks during the "Handegg" phase (Herwegh et al., 2017; Wehrens et al., 2016; Wehrens et al., 2017). The large number and the dispersive distribution of these shear zones in combination with comparatively small offsets of a few centimeters to meters is characteristic and played an important role for the deformation in the sedimentary cover ~~sediments~~. There we find local small-scale folds (Fig. 7e) with a sub~~-~~-vertical axial plane foliation (S2) in the JSW and just above the basement cover contact in the SE. The effect of the "Handegg" phase of vertical tectonics ended in the sedimentary cover units, where the localized shear-zones in the basement were accommodated by (deca)meter-scale folding in the mechanically weaker ~~sediments~~sedimentary rocks (Mid-Jurassic and Triassic; see Sect. 5.3.1 ~~at~~) at their contacts with the basement rock. Therefore, this deformation phase did not affect the sedimentary nappe stack at higher tectonic levels by localized shear deformation (Fig.11b). At the scale of the entire massif, however, the large-scale bulging of both, the basement cover contact and the Helvetic nappe stack is in parts related to this deformation stage.

Subsequent horizontal thrusting overprinted all aforementioned structures, producing a set of thrusts that are found both in the basement and cover rocks (SZ3). These thrusts cut into the ~~sediments~~cover rocks, most notable in the JSW. They further induced the formation of the mylonitic S3 foliation in the ~~sediments~~sedimentary rocks, still under ductile deformation

conditions for calcite. This deformation corresponds to the "Pfaffenchopf" phase of Berger et al. (2017a~~s~~) and Herwegh et al. (2017). It accommodated a significant amount (> 2km in the JSW; Fig. 11) of horizontal displacement, and the deformation was concentrated at several levels. During this phase numerous and large slabs of basement gneisses were wedged into the ~~sediments~~ sedimentary cover (see arrows in Fig. 1~~2~~2~~1~~c). The presence of these has been known for almost a century (e~~i~~.g~~e~~. Scabell, 1926; Collet ~~&~~and Parejas, 1931; Kammer, 1989), yet their origin and particular position has never been considered as a key to understand the deformation style (Fig. 1~~2~~2~~1~~c). ~~These slabs document a significant amount of shortening, which accommodated during the late "Pfaffenchopf" phase of thrusting.~~

5.3.3 Youngest structures

The brittle deformation structures presented in Sect. 4.2 cut all older ones and affect the crystalline basement and the sedimentary cover alike, thus being clearly the youngest ones to be active. The steep NE-SW~~shear zones~~faults (F1~~SZ4~~; Fig. 9b) do not accommodate much offset and rather are present often as open, or partly filled, joint sets. They are strikingly similar to structures reported by Labhart (1966). Berger et al. (2017a) described these structures in the same geodynamic context but referred them as "Gadmen" phase structures. The (sub)vertical SE-NW running ~~planar features~~faults (F2) reported in Sect. 4.2.1 show a complex history of deformation, with clear evidence for brittle deformation (cataclasites of serval generations and young fault gauges in the cores). Offsets at cm to meter scales allow us to identify strike-slip to oblique fault behaviour. They have striking similarities with faults reported from the SW Aar Massif. According to Ustaszewski et al. (2007) these offsets record evidence for "episodic" cycles of brittle deformation and fluid pulses that formed the veins and cataclasites over millions of years. In addition, these faults were considered to offset Quaternary sequences (Ustaszewski et al., 2007) as well. However, both fault sets affect the crystalline basement and the sedimentary cover alike and do not feature large offsets. They are thus not considered as great importance for the structural style and the inferred deformation history.

5.4 Geodynamic implications

The deformation structures described in this work give high resolution insight in the processes that resulted in the exhumation of the ECM to its peculiar position at the Alpine front. First~~T~~, the peak temperature estimations for the internal JSW (<330°C) indicate a depth of 1~~0.5~~1-1~~3~~2 km during these conditions (assuming a geothermal gradient of 27 °C km^{-1}). The onset of dynamic recrystallization in quartz in these rocks indicates that the first deformation occurred close to ~~these~~ peak metamorphic conditions. This deformation produced the fabrics (SZ1, S1), which we link with the imbrication and the stacking of the ~~sediments~~sedimentary strata~~,~~. These processes were ~~which was~~ also associated with the wedging of some basement rock lenses. Hence, t~~T~~his deformation marked the change from thin-skinned tectonics to thick-skinned deformation between 30 and >22 Ma (late "Kiental" phase of Burkhard, 1988) at the external European continental margin. It records the

latest stage of shearing off of sedimentary nappes within the Alpine edifice (Schmid et al., 1996, Handy et al., 2010) ~~It~~ and is ~~characterized~~ dominated by horizontal shortening with a minor vertical component~~and horizontal tectonics~~.

The following drastic change in tectonic style to vertical differential uplift through reverse/normal faulting produced mainly shear zones in the basement (SZ2) with only local folding in the ~~sediments~~ sedimentary cover (~~with~~ axial plane foliation S2). These structures have been related to the "Handegg" phase ~~-~~of deformation (active between 22 and >12 ma), ~~-~~because of their striking similarity with structures in the Haslital and ~~can be found~~ in the entire Aar ~~massif~~ massif (e~~i~~.g~~e~~. Wehrens et al., 2016; Wehrens et al., 2017; Herwegh et al., 2017, Berger et al., 2017a). ~~-~~They accumulate vertical displacement up to 8 km in the southern Aar Massif (Herwegh et al., 2017, Wehrens et al., 2017, Wehrens et al., 2016) while little offset was accumulated ~~It is noteworthy that at~~ in the NW rim of the Aar massif (our study area). ~~little offset was accumulated.~~ The sudden change from horizontal to vertical dominated tectonics ~~was~~ is thought to be induced by buoyancy forces and slab steepening (Herwegh et al., 2017) on a larger scale and ~~was~~ therefore related to the rollback subduction of the European lithospheric mantle slab ~~and slab steepening~~ (Schlunegger ~~&~~and Kissling, 2015; Kissling and Schlunegger, 2018).

Another change in tectonic style (back again to horizontal tectonics) produced the third, more localized deformation fabric (SZ3, S3). This NW directed thrusting ~~occurred during~~cuts and partially overprints older structures, which resembles the "Pfaffenchopf" phase ~~and is an expression of the remaining compressional orogenic forces~~ (Wehrens et al., 2017~~;~~, Herwegh et al., 2017). It is during this phase that a second set of large basement rock slabs ~~is~~ was thrusted into the sedimentary cover. The localized thrust horizons, where ~~One~~ major thrust horizon ~~is~~ located within our JSW, contributed significantly to the uplift during the exhumation. ~~offsetting the EZ for at least 2 km.~~

6 Conclusions

~~We find that linking~~The linkage between the deformation structures in the Aar Massif basement and its sedimentary cover at the Aar Massif NW rim ~~is aggravated~~ allows us to present a detailed picture of how bedrock with different lithologies responded to identical mechanisms under greenschist metamorphic conditions, and lower~~by (i) the different rheological response to strain under the presented T conditions and (ii) the superposition of several deformation structures~~. In this context, we ~~first~~ find that the key for a better understanding of the tectonic complexities lies in the finding ~~that~~ of T_{max} < 330°C. It ~~-~~allows only for brittle deformation of feldspar, dolomite or iron-carbonates, very limited semi-ductile deformation of quartz, and entirely ductile deformation of calcite and phyllosilicates. ~~is key.~~ This leads to ductile folding and thrusting in the calcite-dominated cover ~~sediments~~ rocks (e~~i~~.g~~e~~. Upper Jurassic, Cretaceous) while in the quartz- and feldspar-dominated basement (i.e. the ILZ, EZ) semi-ductile ~~and discrete~~ shear zones were formed ~~whereas~~ despite the bulk of the crystalline basement rock~~s~~ ~~behaved~~ reacts in a brittle manner to the same deformation. ~~Secondly~~Based on this~~,~~ we can disentangle the imprints of at least 3 deformation stages, each leaving different structures in the crystalline basement and the sedimentary cover. This enables us to refine the original 2 phase-subdivision (Kiental- and Grindelwald-phase) and allows us to link our

observations with the recently published large scale block extrusion model of the entire Aar Massif, governed by the change in plate driving forces in the lithospheric mantle. Lastly, we conclude that the ~~multiphase~~multiphase ~~tectonics~~ deformation oriented the basement-cover contact of the Aar Massif in a steep NW plunging manner. The ~~structural imprint~~deformation structures in combination with the uplift (especially the horizontal and vertical shear zones and foliations) set~~s~~ up the stage for preferential erosion to produce the impressive morphology of the Eiger-Jungfrau mountains.

Data availability

Remote sensing derived lineaments used for Fig. 6a are provided as .xyz files with Swiss coordinates (CH1903) ~~are~~ and included in the supplement (S1).
All measured Raman spectra with intensity (in arbitrary units, second column) over Raman shift (in cm-1, first column) and Used spectra for curve fitting (and Fig. S3 histograms) are indicated in the excel sheet, all in the supplement (S2).

Author Contribution

DM and FS designed the study whereas DM and AL carried out fieldwork and LN did the RSCM measurements. DM interpreted the data with additional scientific input from MH. DM prepared the manuscript and figures with contributions from all co-authors.

Acknowledgments

We thank the “Jungfraubahnen” Railway Company, especially Stefan Michel, for their logistic support and access to the railway tunnel. We further thank the High Altitude Research Stations Jungfraujoch and Gornergrat (HFSJG) for making our fieldwork possible. We thank Midland Valley (now Petex) for providing an academic version of Move™, licensed to the Institute for Geological Sciences of the University of Bern. The research was supported by the Swiss National Science Foundation through grant No 159299 awarded to Fritz Schlunegger. Alfons Berger is thanked for discussion about basement rock units. We thank Franz Neubauer and an anonymous referee for insightful comments that improved the manuscript.

Figures and Tables

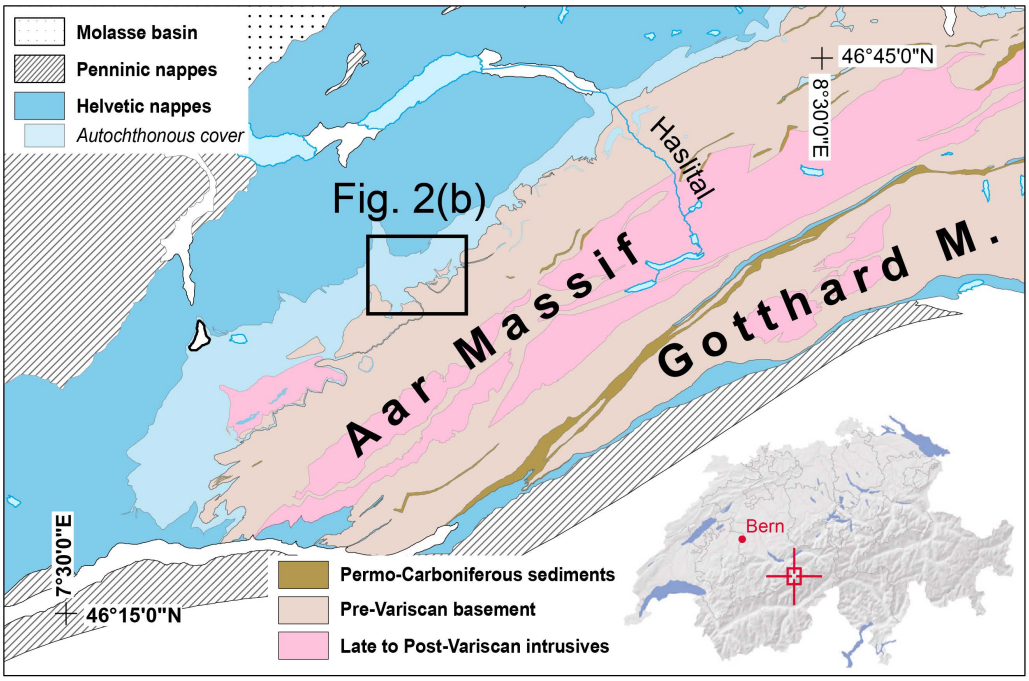

Figure 1. Regional tectonic overview map (modified from Pfiffner et al., 2011) with location of the study area within the Swiss Alps (insert).

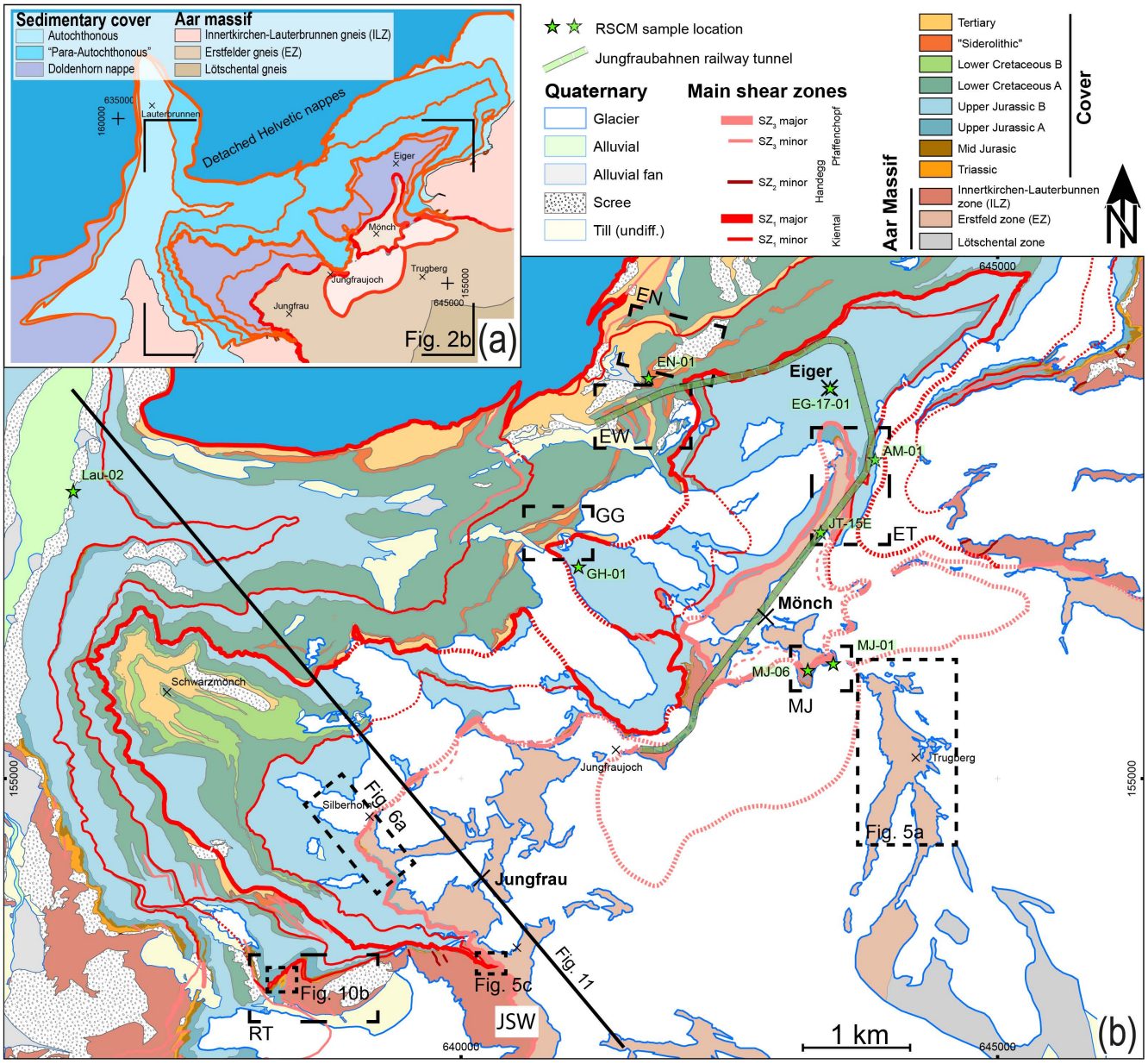

495 **Figure 2. Structural main shear zone map based on own field work and compiled from sources as discussed in Appendix A. (a) Tectonic overview of the studied zone. (b) Refined structural and lithological map. Profile trace for Fig. 11 and key locations (EN… Eiger north, ET… Eismeer/Tunnel, EW…Eiger west, MJ… Moenchsjoch, RT… Rottal, TB… Trugberg; JSW… Jungfrau sediment wedge) are indicated. RSCM sample locations are indicated (subsurface samples from the railway tunnel are indicated with dashed stars). Coordinates are given in Swiss Coordinates (CH1903).**

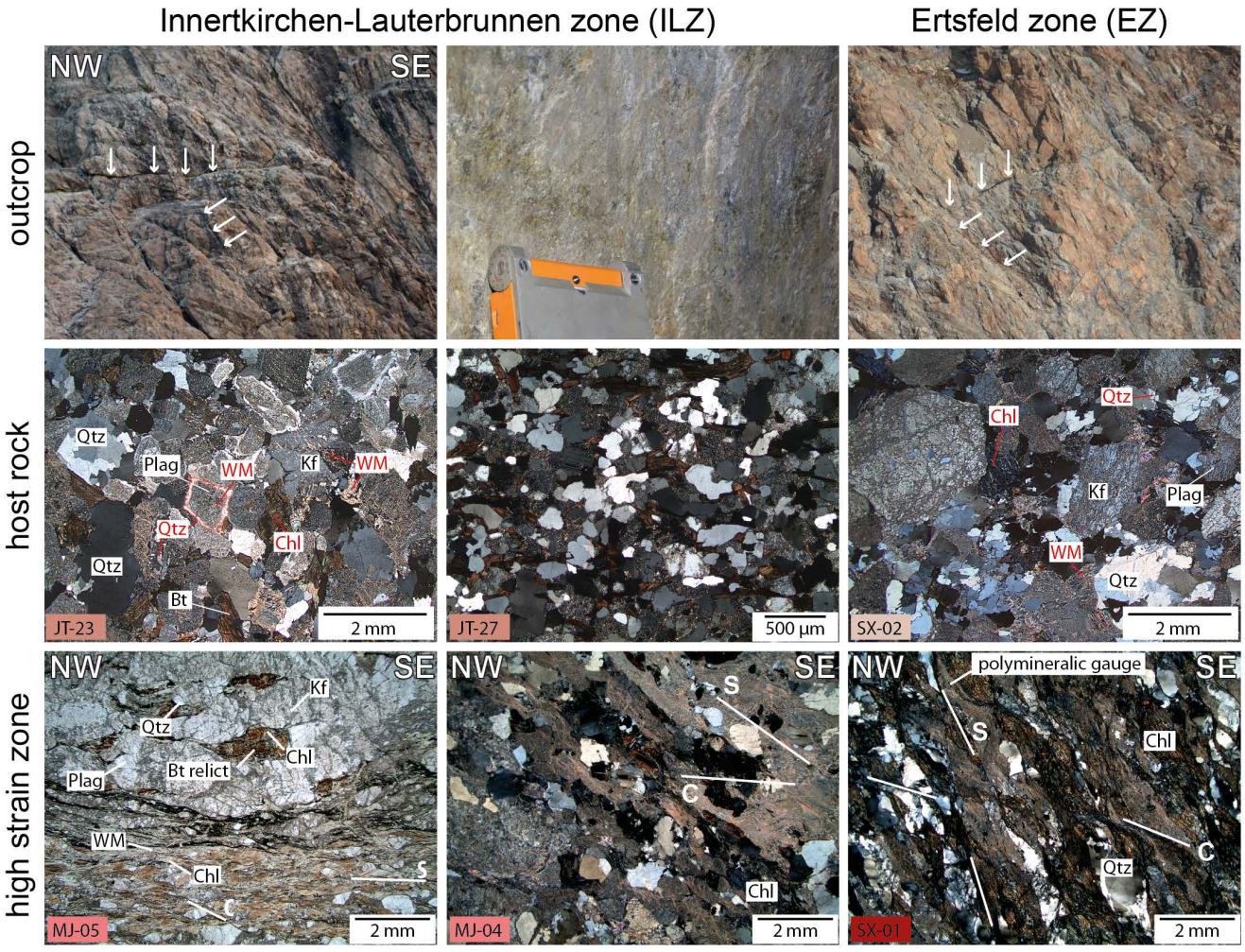

Figure 3. Key basement rock fabrics. Row 1: Outcrop images with indication of discrete shear zones (white arrows). Row 2: Crossed polarized light micrographs of pre-Alpine fabrics with relictic granoblastic microstructures of large feldspar and biotite crystals, and interstitial quartz. Metamorphic overprint manifests in: i) white mica and quartz growth with smaller grain sizes, ii) the alteration rims of feldspar and iii) biotite to chlorite alteration (minerals from overprint are marked in red). Note the highlighted core-rim structure stemming from feldspar sericitization. Row 3: Shear zone micrographs. SC – fabrics are formed by white mica, chlorite and polymineralic fine-grained ultracataclasite or ultramylonite in between porphyroclasts, (which exhibit brittle deformation). Mineral abbreviations: Bt-biotite, Chl-chlorite, Kf-alkali feldspar, Plag-plagioclase, Qtz-quartz, WM-white mica. Sample names are indicated; for sample details see Appendix table A1.

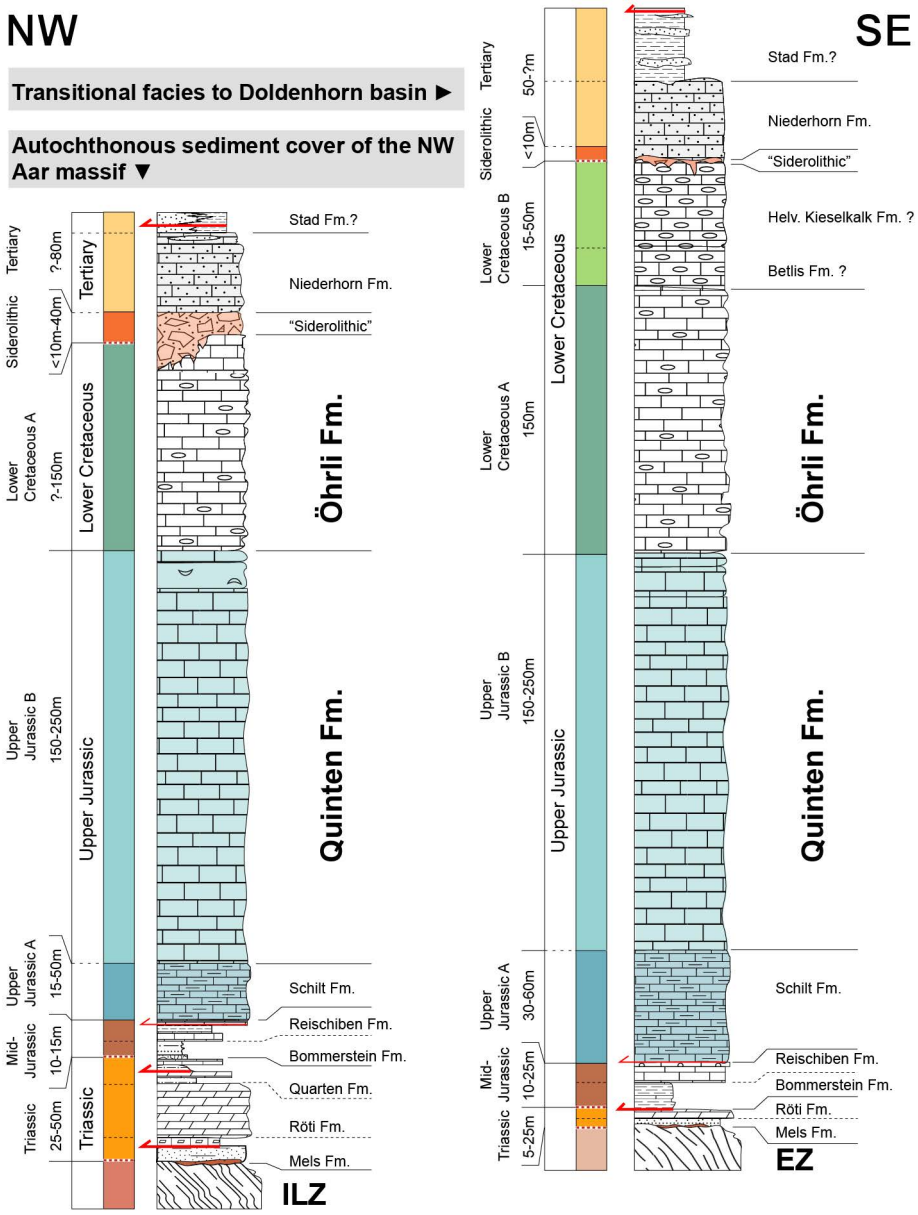

510 **Figure 4. Detailed stratigraphic profiles for the Mesozoic ~~cover~~ sedimentary cover ~~sediments~~ (for sedimentological discussion see Table 2 and Appendix A). Future main detachment horizons are marked (red arrows), ILZ … Innertkirchen-Lauterbrunnen Zone, EZ … Erstfelder Zone. For references for the thickness estimates and individual unit names see table 2. This figure serves as legend for Fig. 110.**

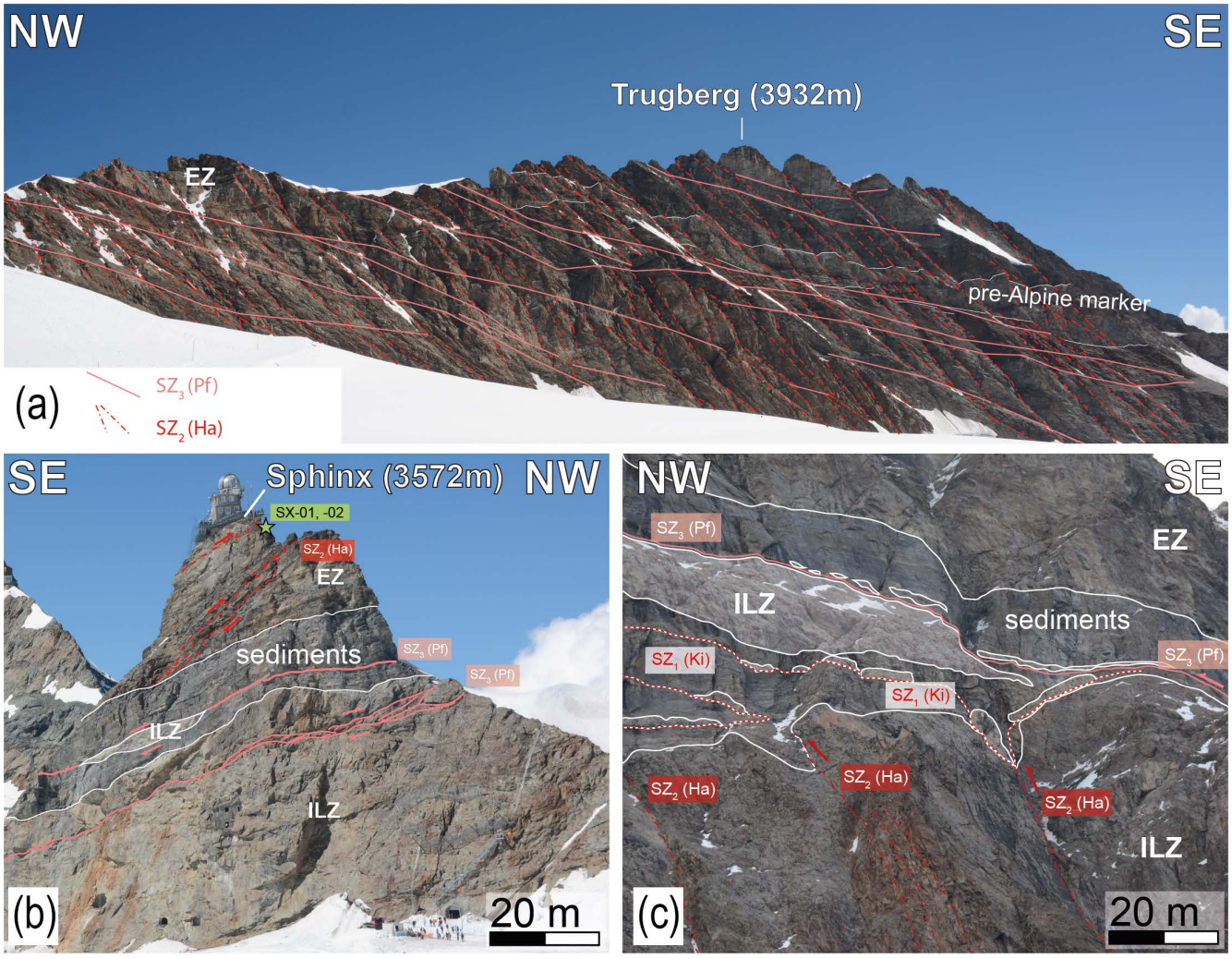

515 **Figure 5. Deformation structures in the basement on the large scale in different key outcrops along the strike of the mountain chain (localities are indicated in Fig. 2). (a) Trugberg mountain ridge viewed from the west: The complex shear zone network with indication of the individual deformation phase structures Pf: Pfaffenchopf phase, Ha: Handegg phase (see also Fig. 6). (b) The Jungfrau sediment wedge (JSW) from the east with an incorporated large basement wedge that separates the Innertkirchen-Lauterbrunnen zone (ILZ) from the Erstfeldzone (EZ). (c) Late stage shear zoning below the Jungfrau demonstrating the complex**
520 **cross-cutting and overprinting relationship of the different structures (Ki: Kiental phase). For deformation phase discussion and attribution see discussion in text. Location of key samples is indicated (SX-01, SX-02).**

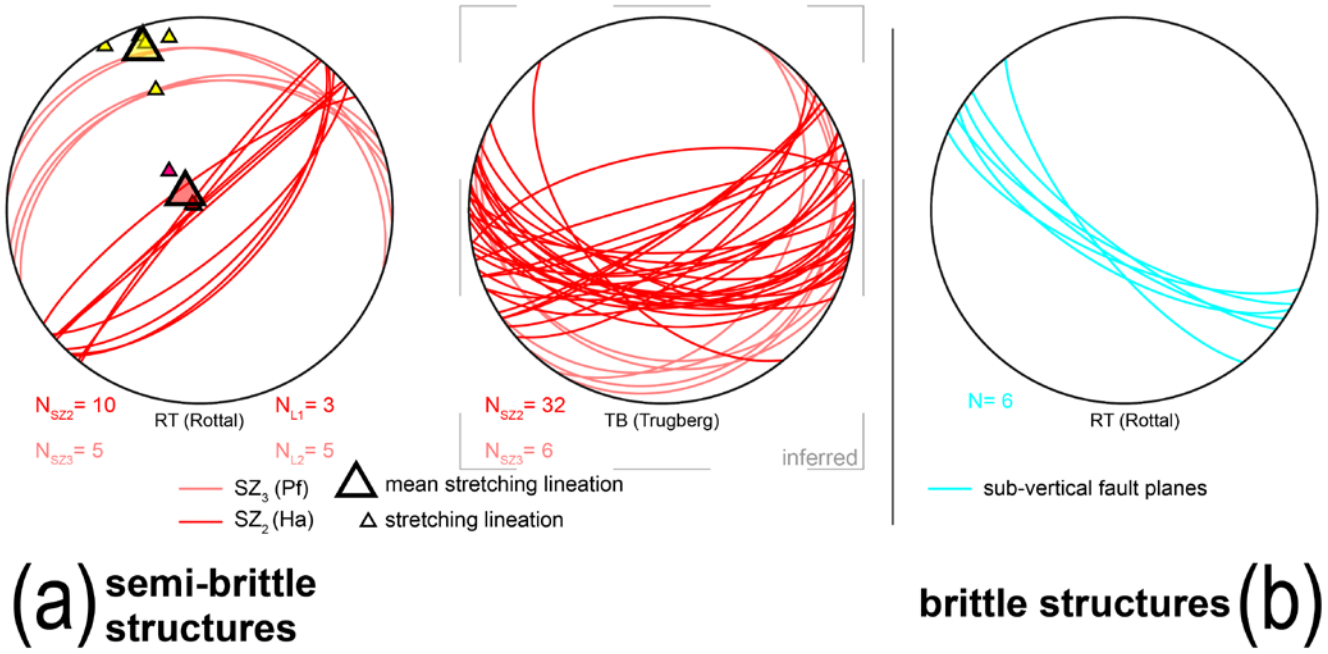

Figure 6. Structural field data for the basement from the Rottal (RT). (a) Shear zones related to main phases of exhumation. Shear zone orientations for TB were inferred from by plane fitting through moment of inertia of remote sensed lineaments (data provided in the supplement S1). (b) Vertical lineaments that crosscut structures from (a). For geographical abbreviations and shear zone legend see Fig. 2.

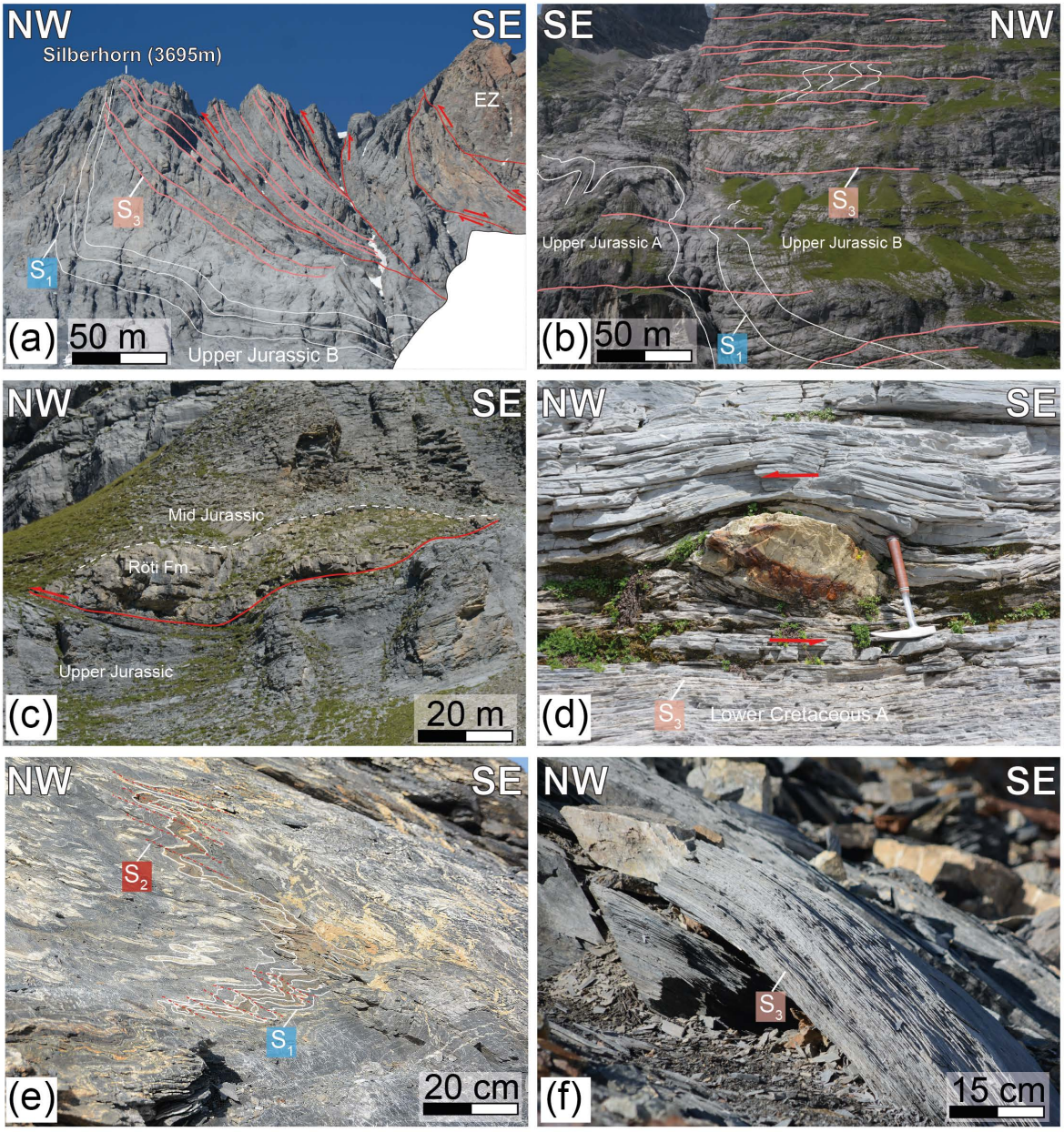

Figure 7. Field examples of key deformation structures within the ~~sediments~~sedimentary rocks. (a) Modulation of the previous foliation (S1, white lines) by the latest stage fault system (solid red lines) and the contemporarily induced foliation (S3, pink lines) in the summit region of the Jungfrau. (b) Similar overprinting of already folded bedding by the younger foliation east of the Eiger summit in a lower level (elevation around 2500m a.s.l). (c) Decameter size dolomite boudin of the Triassic (Roeëti Fm.) marking the shear zone at its base in the RT (Rottal) region, which is the roof thrust of the autochthonous cover unit. (d) Decameter sized sigma clasts of boudinaged iron-rich nodules ("Siderolithic" Fm.) within the ductile host rock mylonites that marks a shear zone in the west flank of the Eiger Mountain. (e) Local modulation of the initial foliation and folds by steep SE plunging axial planes with foliation, inflicted during the intermediate step of deformation (Ha). (f) Carbonaceous ultramylonite in the MJ transect, some

decameter above the location of (e), showing the strongly localized latest overprint, completely ~~removing~~ transposing traces of previous deformation.

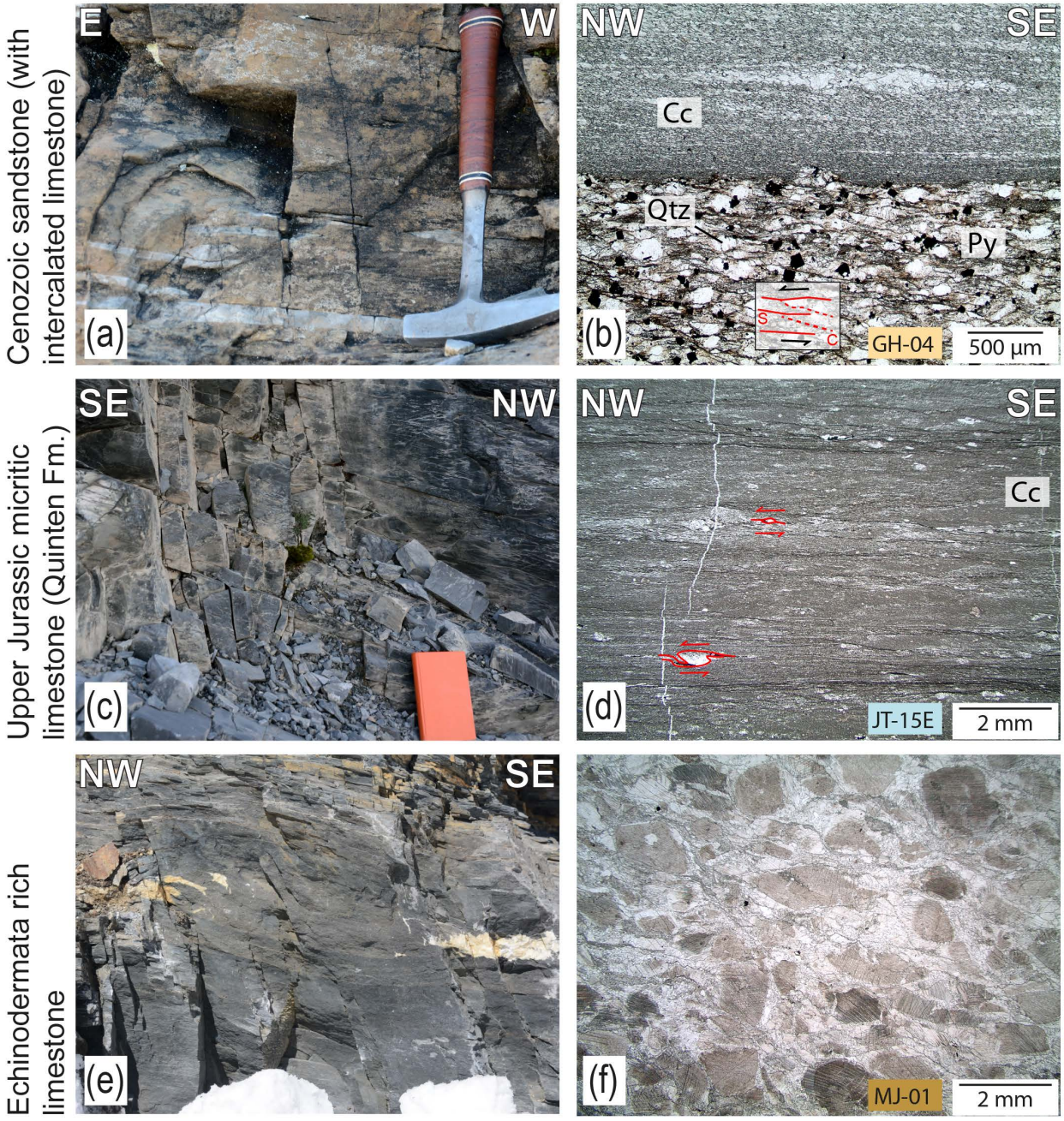

Figure 8. Deformation structures on outcrop and microscale. (a) Ultra-mylonitic Tertiary sandstones intercalated with calcite limestones that (b) show a dynamically recrystallized fabric in the limestone part, while the quartz within the S-C mylonite exhibits still (semi) brittle behavior. This manifests in mylonitic ductile shear bands formed by micas and calcite while quartz grains (along with p~~P~~yrite) form sigmoidal clasts. (c) Dark ~~and~~ micritic limestone mylonites of the Upper Jurassic B unit with a

(d) completely recrystallized fabric of microcrystalline calcite. (e) Echinodermata-rich limestone of the Mid Jurassic show the low P, T overprint with (f) un-deformed echinodermatas, probably due to consisting of Mg- calcite and thus being stronger (Xu et al., 2009). Mineral abbreviations: Cc-calcite, Qtz-quartz, Py-pyrite.

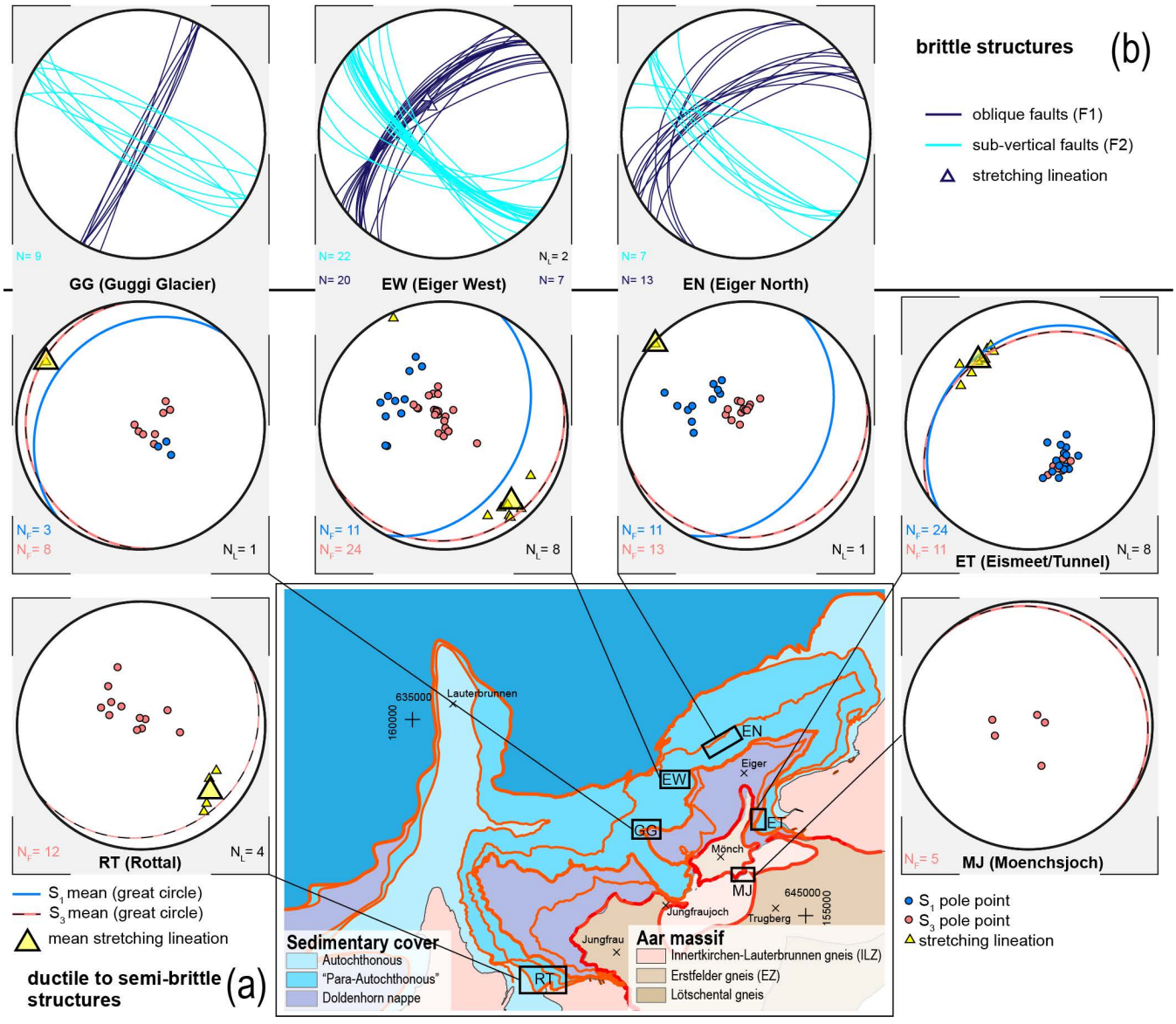

Figure 9. Deformation structures in the sediments. (a) Bedding parallel S1 foliation and later induced S23 foliation that consists of numerous slip surfaces. Stretching lineation are only documented on S32 surfaces. (b) Brittle-only structures that crosscut structures in (a).

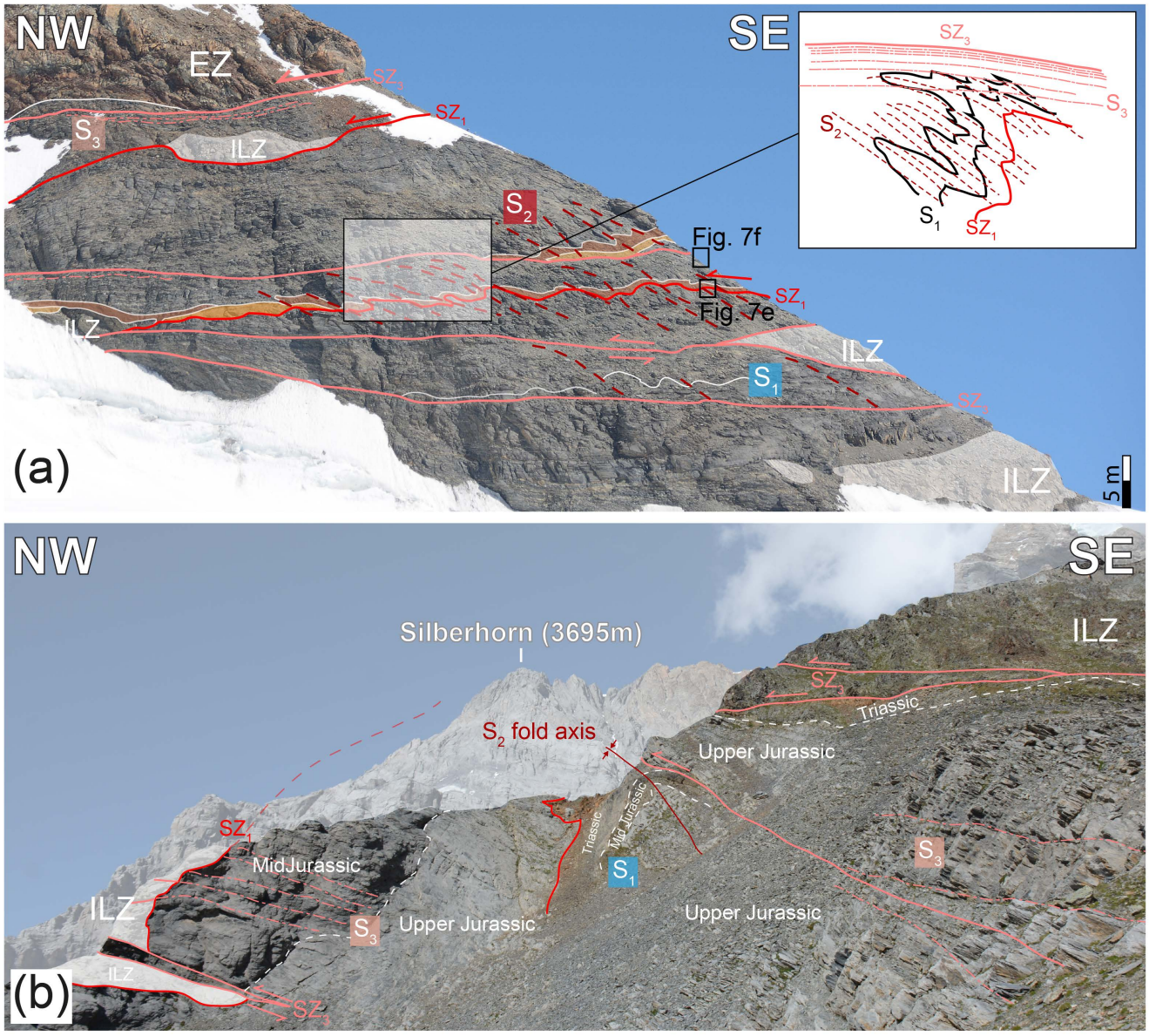

Figure 10. Cross-cutting and overprinting relations between the structures close to the basement cover contact for key locations. (a) Sediments in the Jungfrau sediment wedge (JSW), at the Moenchsjoch locality (MJ; see Figs. 2,9), between the Erstfelder gneiss zone (EZ) and the Innertkirchen-Lauterbrunnen zone (ILZ) illustrating the crosscutting and overprinting (see also insert). Note that some sediment markers are highlighted (brown: Mid-Jurassic, orange: Triassic). (b) Similar structures at the Rottal (RT; see Figs. 2,9) location, where the late thrusting of the ILZ basement caused deflection and rotation of the S2 folds and cross-cutting and passive rotation of the SZ1 thrusts. Note the penetrative S3 foliation.

560

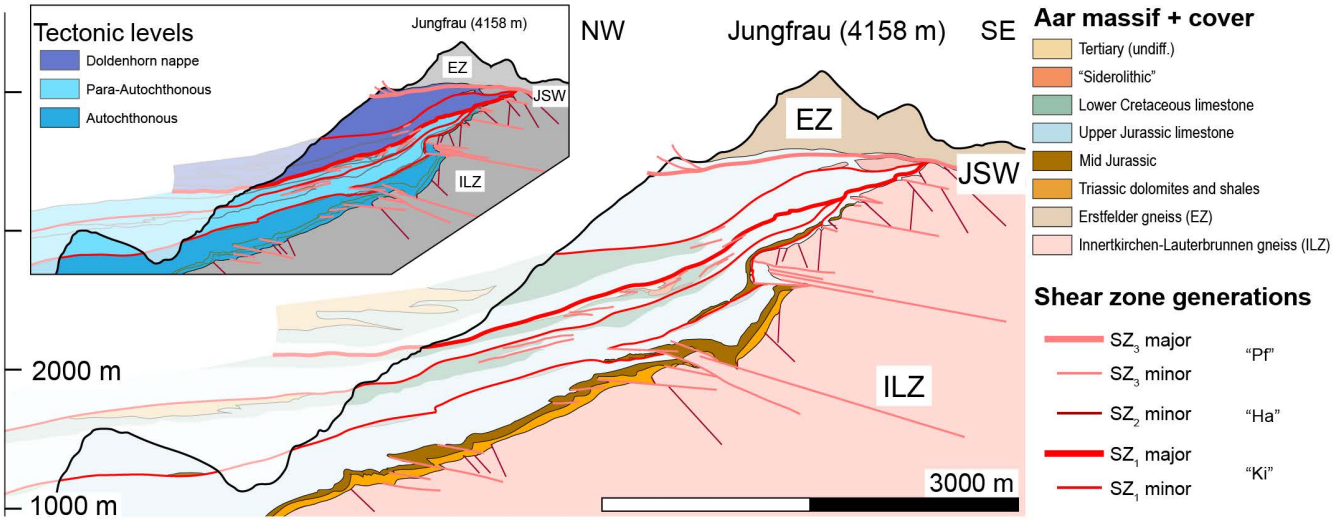

Figure 110. Simplified structural profile across the NW rim of the Aar Massif (profile trace indicated in Fig. 2).

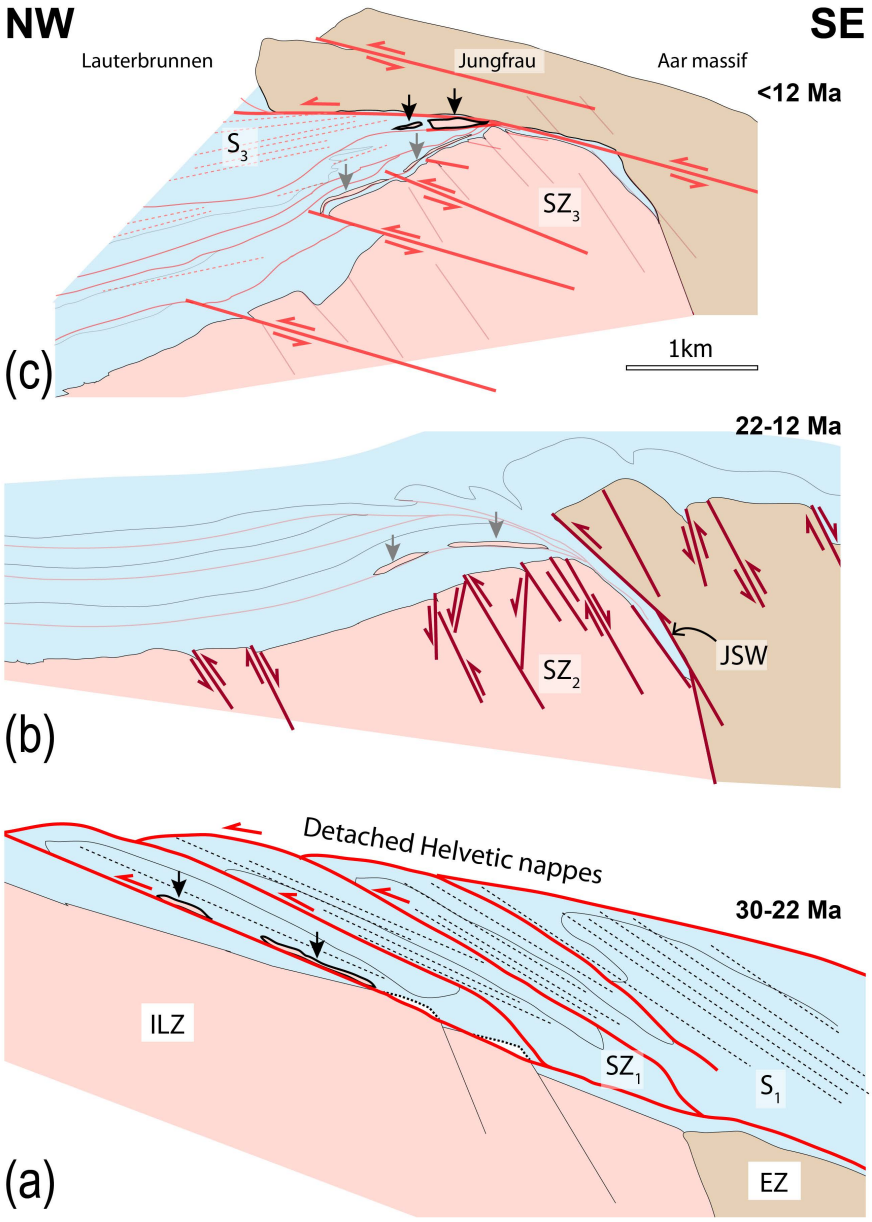

Figure 12~~1~~. Schematic sketch of the evolution during the main deformation stages of the Alpine evolution. (a) In sequence imbricate stacking during the late Kiental phase that induced S1 foliation and led to the incorporation of basement slabs into the sediment stack (black arrows). (b) Steep reverse faulting of SZ2 that induced folding in the cover during the Handegg phase. (c) SZ3 thrusts and S3 foliation in the ~~sediments~~ sedimentary cover during the Pfaffenchopf phase along with second generation of basement slabs incorporated into the ~~sediments~~ sedimentary cover (black arrows).

Age [Mma]	Main phase	Sub-stage	Domain	Main characteristics	References
30-22	**Kiental**		West Helvetics	Nappe stacking with folding	Burkhard (1988)
20-?	**Grindelwald**		Central Helvetics	Passive rotation and folding	Burkhard (1988), Pfiffner (2014)
22->1220		Handegg	Aar Massif	Steep normal/reverse faults	Wehrens et al. (2016), Berger et al. (2017a)
20-17		Oberaar	South Aar Massif	Dextral/oblique strike slip faults	Wehrens et al. (2016)
<12		Pfaffenchopf	NW Aar Massif	Flat reverse/normal faults	Wehrens et al. (2017)
< 5?		Gadmen	NW Aar Massif	Steep brittle reverse faults	Berger et al. (2017ab) ~~Herwegh et al. (in review)~~

Table 1. Compilation of deformation phases from literature.

Simplified layer	Fm. Name	Age	Lithology	References	Thickness constraint
Tertiary	Stad Fm.	Priabonian	Shales intercalated with sandy layers/lenses	Herb (1983), Menkveld-Gfeller et al. (2016)	n/a
	Niederhorn Fm.	Bartonian – Priabonian	Shallow marine limestones, intercalated with sandstones	Herb (1983), Menkveld-Gfeller et al. (2016)	n/a
"Siderolithic"	"Siderolithic"	Lutetian – Bartonian	Erosional infill in karst pockets (sandstones, iron rich carbonates) &and calcareous breccia	Menkveld-Gfeller et al. (2016)	<10m to 40m
Lower Cretaceous B	Betlis Fm./ Helv. Kieselkalk (?)	Valanginian	Brown weathering biogene spary limestone with chert layers and sandy layers in the top	Strasser (1982), this study	50 to 90 m
Lower Cretaceous A	OeÖhrli Fm.	Berriasian	Light grey, oolithic – biogene limestones		? to 150 m
Upper Jurassic B	Quinten Fm.	Oxfordian - Berriasian	Dark, micritic limestones; on top reef platform limestones	Collet &and Parejas (1931), Masson et al. (1980)	150 to 250 m
Upper Jurassic A	Schilt Fm.	Callovian – Oxfordian	Intercalated limestones with thin marly layers		10 to 50 m
Mid Jurassic	Reischiben Fm.	Aalenian – Bathonien	Echinoderm bearing calcareous breccia and Iiron bearing sandstones	Bruderer (1924)	<1 to 10 m
	Bommerstein Fm.	Toarcian – Aalenian	Shales with intercalated iron rich sandstones and echinoderm bearing calcareous breccia	Bruderer (1924)	<1 to 30 m
Triassic	Quarten Fm.	Late Triassic		Bruderer (1924), this study	n/a
	Roeëti Fm.	Anisian	Dolomoites: pseudomorphs after gypsum, oolithic grainstones and mudstones; well-bedded	Gisler et al. (2007), Collet &and Parejas (1931), Rohr (1926)	5 to 25 m
	Mels Fm.	Olenekian — Anisian	Intercalated Ssandstones, clays and dolomites (partly anhydrous gypsum bearing)	Gisler et al. (2007), Rohr (1926), this study	< 10m
n/a	n/a	Permian?	Regolith (weathered Permian basement rock)	this study	< 5m

Table 2. Key stratigraphic horizons with most important features and references (for a detailed discussion see Appendix A).

Sample	x	y	Elev. [m]	stratigraphic unit	tectonic unit	RSCM-T [°C]		2σ
MJ-01	643469	156074	3649	Mid Jurassic	JSW	308	±	14
MJ-06	643232	156012	3744	Upper Jurassic A	JSW	317	±	11
EN-01	641749	158733	2388	Lower Cretaceous A	PA	283	±	12
Lau-02	636387	157680	838	Upper Jurassic B	AUT	283	±	11
EG-17-01	643440	158638	3970	Upper Jurassic B	DN	292	±	10
JT-15E	643351	157295	3216	Upper Jurassic B	PA	287	±	14
AM-01	643859	157971	3127	Upper Jurassic B	PA	307	±	19
GH-01	641095	156976	2798	Upper Jurassic B	DN	289	±	27

575 **Table 3. RSCM results for peak metamorphic temperature estimation … Jungfrau shear zone, PA ... "Para-Aautochthonous" sediments, DN… Doldenhorn nappe, AUT … Autochthonous sediments. Coordinates are given in Swiss coordinate system, (CH1903).**

Appendix A: Geological map compilation and Mesozoic litho-stratigraphy.

The structural map (Figs. 1 ~~&~~and 10) was compiled from the following preexisting maps: Collet and Paréjas (1928), Günzler-Seifert ~~&~~and Wyss (1938) and the GeoCover maps: LK 1228, 1229, 1248, 1249 which in turn largely base on the former publications. The most recent maps of Pfiffner et al. (2011) and Berger et al. (2017b), which present the geological architecture at a regional scale, were considered as well. A set of profiles produced by Collet ~~&~~and Paréjas (1931) and Günzler-Seifert ~~&~~and Wyss (1938), Herb (1983) and Hänni ~~&~~and Pfiffner (2001) was used as a basis. However, the first sections by Collet ~~&~~and Paréjas (1931) and Günzler-Seifert ~~&~~and Wyss (1938) have not been geo-referenced, with the consequence that the course of the section cannot be precisely allocated. Therefore, these profiles had first to be homogenized in structural style, geo-referenced and integrated in our updated geological map.

The paleo-geographical northwestern late Permian to early Triassic strata (Fig. 4) has been assigned to a terrestrial flood plain environment where the sediments were directly deposited on the weathered crystalline basement (Mels Fm.). This unit is then overlain by mixed siliciclastic-carbonaceous ~~sediments~~ sediments and a sequence of dolomites, thus marking a tidal flat, Sabkha-type of environment (R~~ö~~oeti Fm.; Gisler et al., 2007). These ~~early~~ Lower Triassic ~~sediments~~ sedimentary rocks are preserved as quartzite, slate and dolomite (locally anhydrite bearing in the Roe~~ö~~ti and Mels Fm.). In the lowest tectonic level (= the cover of the most external part of exhumed the Aar situated in the Lauterbrunnen valley) an up to 30m thick suite of dolomites overlain with a suite of shales with up to 5 m thick dolomite beds, which have been assigned to the Roe~~ö~~ti and Quarten Fm., is preserved (Bruderer 1924). These ~~sediments~~ sedimentary rocks (and possibly overlying units) were subject to erosion during the ~~Upper~~ Late Triassic/~~Lower~~ Early Jurassic. This is recorded by < 1-m thick breccias ("Basalbreccie") containing Roe~~ö~~ti dolomite components (Krebs 1925; Frey 1968). After the hiatus, a thin succession of ferrous sandstones intercalated with echinoderm-rich limestones was deposited. This unit, which have been assigned to the Bommerstein Fm. and Reischiben ~~Fm. and~~Fm. ~~-~~are <10 m thick at the base of the Lauterbrunnen valley (Masson et al., 1980; Collet ~~and&~~ Paréjas, 1931) also contain a thin oolithic horizon that contains iron- and manganese-rich concretions. This formation is overlain by a suite of cm- to dm-thick bedded, sandy to argillaceous limestones (Schilt Fm.).

These are gradually replaced a the dark, micritic limestone upsection, referred to as the Quinten Fm. Deposition of this latter unit commenced in the lower Oxfordian and reaching an estimated thickness between 75m ~~to~~ and 150m in the study area (Collet ~~&~~and Paréjas, 1931). The Quinten unit itself is overlain by fossil-rich limestones (Oe~~Ö~~hrli Fm.) of varying thicknesses. These differences in preserved thicknesses are due to a Tertiary phase of erosion where stratigraphic columns were dissected to successively deeper levels from the NW to the SW. Iron-rich sandy to argillaceous infills in karst pockets combined with a few meters' thin horizon of iron rich sandstones are documents of this erosional phase. Related fragments, most likely of pre-Priabonian to Eocene age, are referred to as the "Siderolithikum" (Herb 1983; Wieland 1979). Locally it forms up to a 40 m-thick suite of breccias with components of Quinten-limestone, Oe~~Ö~~hrli-limestone and "Helvetischer Kieselkalk" (Wieland 1979). The overlying calcareous breccia, known as "Mürren-Brekzie" with thicknesses of up to 80 m in the Eiger north face (Günzler-Seifert ~~&~~and Wyss, 1938; Collet ~~&~~and Paréjas, 1931), already chronicles the Priabonian

transgression resulting in the deposition of the Niederhorn Fm. This unit is considered as equivalent of the Hohgant Sandstone Member (Menkveld-Gfeller et al., 2016). These clastic shoreface deposits are overlain by a limestone suite referred to as the "Lithothamnienkalke" (Menkveld-Gfeller, 1994). Sandstone lenses and dark bituminous carbonates (most likely Gemmenalp limestone equivalents) become more frequently upsection and grade into a succession of marls alternated with siliciclastic turbidites and calciturbidites. These ~~sediments~~ rocks were mapped as "Flysch" (Collet ~~&~~and Paréjas, 19312~~8~~), but we note here they have striking similarities with ~~sediments~~ sedimentary rocks in the flank of the Schwarzm~~ö~~oench, the depositional ages of which have tentatively been assigned to the Priabonian (Günzler-Seifert ~~&~~and Wyss, 1938). Hence it is debatable whether the attribution to the Stad Fm. or to the North Helvetic flysch group is correct.

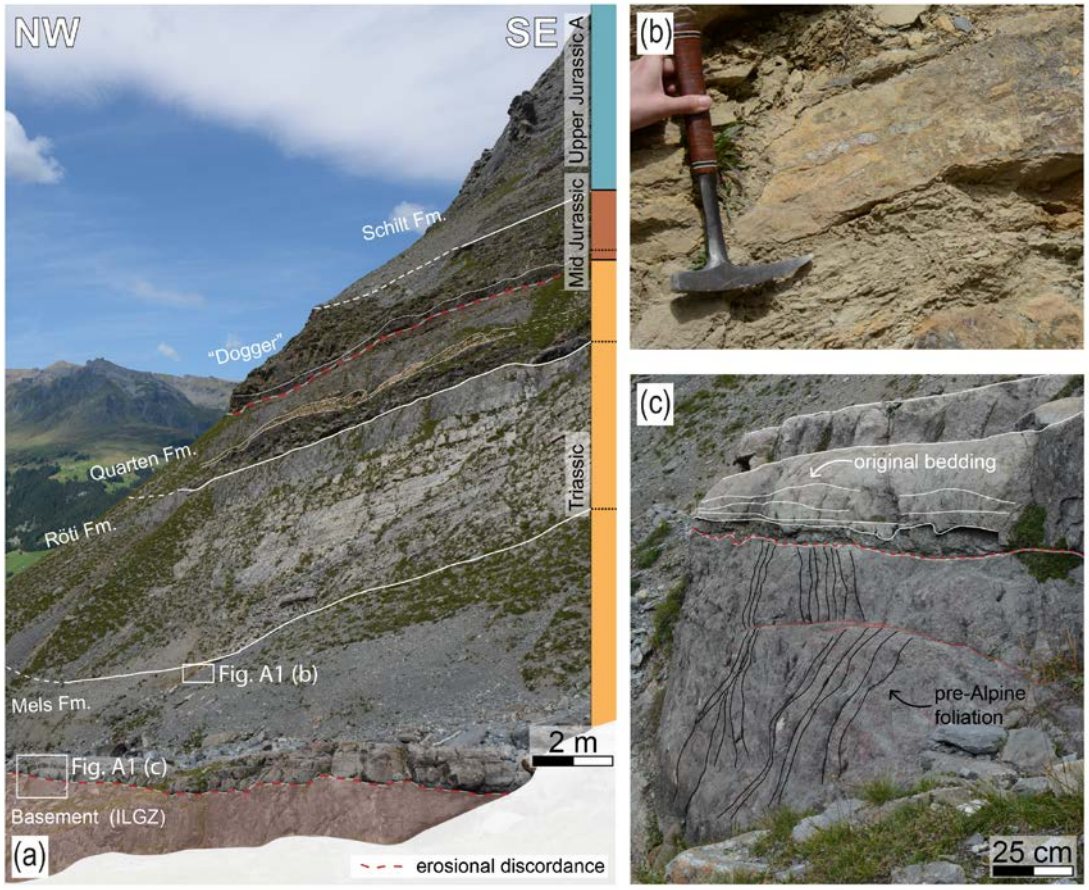

Figure A1. Undeformed basal stratigraphic section of the sedimentary cover ~~sediments~~ of the ILZ in the Rottal (RT).

Within the Jungfrau sediment wedge (JSW), the sedimentary succession (Fig. 4) starts with a < 1 m-thick Permian paleosol, which has also been encountered farther to the west (Krayenbuhl ~~&~~ and Steck, 2009). This is overlain by Triassic slates and sandstones attributed to the Mels ~~f~~Formation~~m~~., and a < 2 m-thick sequence of dolomites (Roe~~ö~~ti Fm.). Similar to the situation of the Autochthon, no ~~u~~Upper Triassic ~~sediments~~ rocks are present, either due to non-sedimentation or to a phase of

post-depositional erosion lasting until the Middle Jurassic (Masson et al., 1980). The succession of echinoderm-rich and iron-manganese-nodules, deposited during middle-Jurassic times (Bommerstein Fm. and Reischiben Fm.), are considerably thicker than in the NW. This supports the inferred strong tectonic thinning of this unit (~10 m at Moeënchsjoch, MJ; ~5 m at the Eismeer ET; Collet & and Paréjas 1931). Similarly, the overlying sandy limestones of the Schilt Fm. are still thicker than 30 m (Fig. 3). The Upper Jurassic to Cretaceous limestones of the Quinten and OeÖhrli Formations are generally missing within the JSW and have been displaced to the NW. As a consequence, they can be found in the middle part of the Eiger (Fig. 2), above the Eismeer/Tunnel (ET) area and in the northern flank of the Mëoench (Fig. 2). The entire sedimentary stack is strongly folded, foliated and thrusted, which leads to a doubling and to an inversion of the upper part, while the succession has been repeatedly stacked in other localities.

Sample	x	y	Elev.	rock type	Domain	Qtz rec.	mica dominance	Mica in SZ	Def. structures	SZ generation
JT-23	642048	155392	3388	gneisgneiss (polymetamoprh)	ILZ (tunnel)	n/a	WM>Chl>Bt	n/a	n/a	n/a
JT-27	641960	155313	3417	gneisgneiss (polymetamoprh)	ILZ (tunnel)	n/a	WM, Bt	n/a	n/a	n/a
MJ-04	643499	156091	3647	gneisgneiss mylonite	ILZ	BLG	Chl	WM	mica shear bands	SZ3
MJ-05	643232	156012	3744	gneisgneiss mylonite	JSW	BLG	Chl	Chl	mica shear bands	SZ3
SX-01	641944	155292	3565	gneisgneiss mylonite	EZ	BLG	WM, Chl	WM	mica shear bands	SZ2
SX-02	641944	155292	3565	gneisgneiss (polymetamoprh)	EZ	BLG	WM	n/a	n/a	n/a
GH-01	641095	156976	2798	Calcite/sandstone mylonite	Tertiary	n/a	WM	WM	Cc regrowth; SC, fabrics	S1, S3
JT-16E	643351	157295	3215	Calcite mylonite	Upper Jurassic A	n/a	n/a	n/a	Cc regrowth	S1, S3
MJ-01	643469	157295	3215	Echinodermata-bearing breccia	Mid Jurassic	n/a	n/a	n/a	SC fabrics	S1, S2, S3

Table A1. Basic data for selected samples used in Figs. 3 &and 8. Thin section description for dominant dynamic quartz recrystallization mechanism (BLG… bulging), dominant mica and mica growth in shear zone (if applicable). For shear zone generation discussion see Sect. 4.2.1.

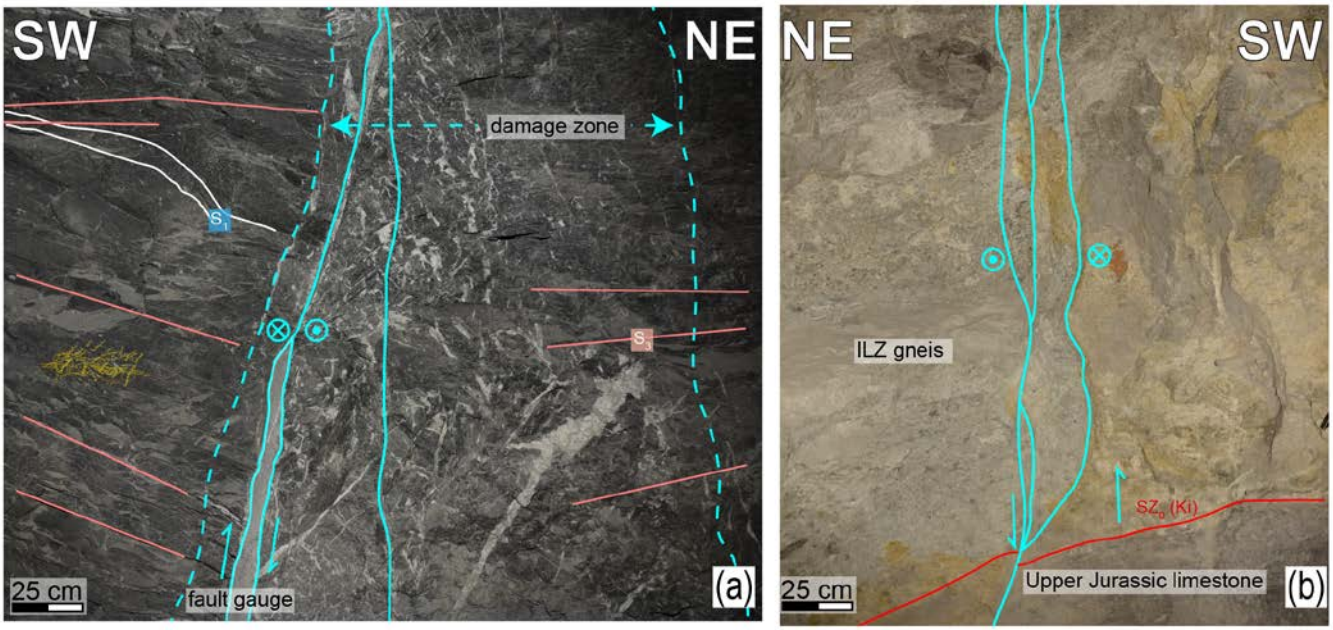

640 **Figure A2. Youngest fault structures (F2) cross-cutting all previous structures in the ~~sediments~~ sedimentary cover (a) and the basement (b) with an oblique to strike-slip behavior.**

Appendix B: RSCM temperature estimate histograms

Fitted Raman spectra distributions (Fig. B1) display reasonable gaussian probability distributions with max. spread of 50°C (except for GH-01).

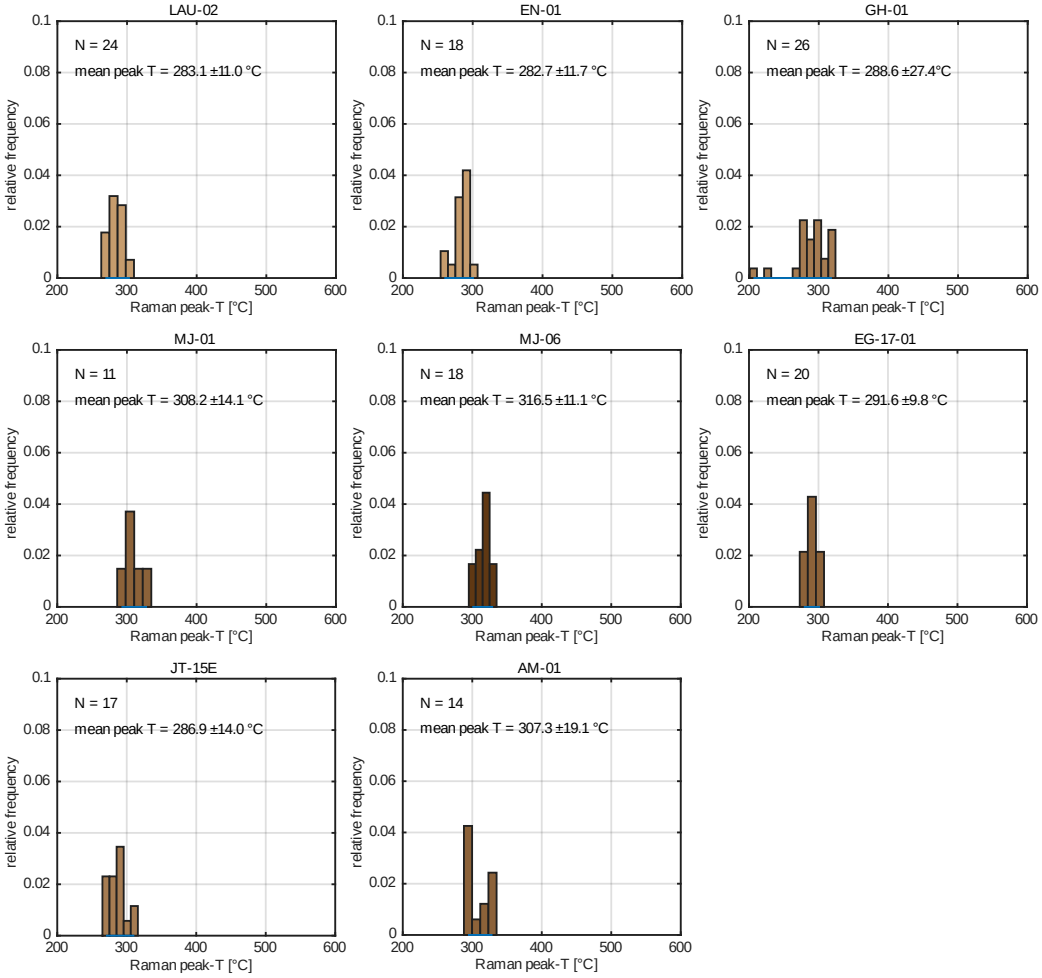

Figure B1. RSCM temperature estimate histograms for each sample for the fitted spectra.

References

Abrecht, J.: Geologic units of the Aar massif and their pre-Alpine rock associations: a critical review, Schweizerische Mineral. und Petrogr. Mitteilungen, 74, 5–27, doi:10.5169/seals-56328, 1994.

Baltzer, A.: Der mechanische Contact von Gneiss und Kalk im Berner-Oberland, Dalp, Bern, 255 pp, 1880.

Bambauer, H. U., Herwegh, M. and Kroll, H.: Quartz as indicator mineral in the Central Swiss Alps: the quartz recrystallization isograd in the rock series of the northern Aar massif, Swiss J. Geosci., 102, 345–351, doi:10.1007/s00015-009-1319-z, 2009.

Baumberger, R., Herwegh, M., Kissling, E. Remote sensing and field data based structural 3D modelling (Haslital, Switzerland) in combination with uncertainty estimation and verification by underground data. AGU Geophysical Monographs, in press.

Berger, A., Wehrens, P., Lanari, P., Zwingmann, H. and Herwegh, M.: Microstructures, mineral chemistry and geochronology of white micas along a retrograde evolution: An example from the Aar massif (Central Alps, Switzerland), Tectonophysics, 721, 179–195, doi:10.1016/j.tecto.2017.09.019, 2017a.

Berger, A., Mercolli, I., Herwegh, M., and Gnos E.: Geological Map of the Aar Massif, Tavetsch and Gotthard Nappes 1:100 000, ISBN 978-3-302-40093-8, 2017b.

Beyssac, O., Goffé, B., Chopin, C. and Rouzaud, J. N.: Raman spectra of carbonaceous material in metasediments: a new geothermometer, J. Metamorph. Geol., 20, 859–871, doi:10.1046/j.1525-1314.2002.00408.x, 2002.

Bruderer, W.: Les sédiments du bord septentrional du Massif de l'Aar du Trias à l'Argovien: Thèse Sc. Lausanne 86p, 1924.

Burkhard, M.: L'Helvétique de la bordure occidentale du massif de l'Aar (évolution tectonique et métamorphique), Eclogae Geol. Helv., 81, 63–114, doi:10.5169/seals-166171, 1988.

Burkhard, M.: Calcite twins, their geometry, appearance and significance as stress-strain markers and indicators of tectonic regime: a review, J. Struct. Geol., 15(3–5), 351–368, doi:10.1016/0191-8141(93)90132-T, 1993.

~~Burkhard, M.: Ductile deformation mechanisms in micritic limestones naturally deformed at low temperatures (150–350°C), Geol. Soc. London, Spec. Publ., 54, 241–257, doi:10.1144/GSL.SP.1990.054.01.23, 1990.~~

Challandes, N., Marquer, D. and Villa, I. M.: P-T-t modelling, fluid circulation, and 39Ar-40Ar and Rb-Sr mica ages in the Aar Massif shear zones (Swiss Alps), Swiss J. Geosci., 101, 269–288, doi:10.1007/s00015-008-1260-6, 2008.

Collet, L. and Paréjas, E.: Géologie de la chaîne de la Jungfrau, Beiträge zur Geol. Karte der Schweiz, n.s. 63, 1931.

Escher von der Linth, A.: Erläuterung der Ansichten einiger Contact-Verhältnisse zwischen Krystallinischen Feldspathgesteinen und Kalk im Berner Oberland, 13p, doi:10.3931/e-rara-19223, 1839.

Fernández, O.: Obtaining a best fitting plane through 3D georeferenced data, J. Struct. Geol., 27, 855–858, doi:10.1016/j.jsg.2004.12.004, 2005.

Frey, M. and Mählmann, F.: Alpine metamorphism of the Eastern. Schweizerische Mineral. und Petrogr. Mitteilungen, 79, 135–154, doi:http://doi.org/10.5169/seals-60202, 1999.

Gisler, C., Hochuli, P. A., Ramseyer, K., Bläsi, H. and Schlunegger, F.: Sedimentological and palynological constraints on the basal Triassic sequence in Central Switzerland, Swiss J. Geosci., 100, 263–272, doi:10.1007/s00015-007-1225-1, 2007.

Glotzbach, C., Reinecker, J., Danišík, M., Rahn, M., Frisch, W. and Spiegel, C.: Thermal history of the central Gotthard and Aar massifs, European Alps: Evidence for steady state, long-term exhumation, J. Geophys. Res., 115(F3), F03017, doi:10.1029/2009JF001304, 2010.

Günzler-Seifert, H. and Wyss, R.: Erläuterungen zum Kartenblatt Grindelwald, Geol. Kommision der schweiz. Naturforsch. Gesellschaft, 1938.

Haertel, M. and Herwegh, M.: Microfabric memory of vein quartz for strain localization in detachment faults: A case study on the Simplon fault zone, J. Struct. Geol., 68, 16–32, doi:10.1016/j.jsg.2014.08.001, 2014.

Handy, M. R., M. Schmid, S., Bousquet, R., Kissling, E. and Bernoulli, D.: Reconciling plate-tectonic reconstructions of Alpine Tethys with the geological–geophysical record of spreading and subduction in the Alps, Earth-Science Rev., 102(3–4), 121–158, doi:10.1016/j.earscirev.2010.06.002, 2010.

Herb, R.: Bericht über die Exkursion der Schweizerischen Geologischen Gesellschaft auf das Schilthorn vom 19. September 1982, Eclogae Geol. Helv., 76, 181–188, doi:10.5169/seals-165356, 1983.

Herwegh, M. and Pfiffner, O. A.: Tectono-metamorphic evolution of a nappe stack: A case study of the Swiss Alps, Tectonophysics, 404, 55–76, doi:10.1016/j.tecto.2005.05.002, 2005.

Herwegh, M., de Bresser, J. H. P. and ter Heege, J. H.: Combining natural microstructures with composite flow laws: an improved approach for the extrapolation of lab data to nature, J. Struct. Geol., 27, 503–521, doi:10.1016/j.jsg.2004.10.010, 2005.

Herwegh, M., Berger, A., Baumberger, R., Wehrens, P. and Kissling, E.: Large-Scale Crustal-Block-Extrusion During Late Alpine Collision, Sci. Rep., 7, 413, doi:10.1038/s41598-017-00440-0, 2017.

Kammer, A.: Alpidische Verformung des aarmassivischen Nordrandes, Schweizerische Mineral. und Petrogr. Mitteilungen, 69, 37–53, doi:10.5169/seals-52775, 1989.

Kennedy, L. A. and White, J. C.: Low-temperature recrystallization in calcite: Mechanisms and consequences, Geology, 29(11), 1027, doi:10.1130/0091-7613(2001)029<1027:LTRICM>2.0.CO;2, 2001.

Kissling, E. and Schlunegger, F.: Rollback Orogeny Model for the Evolution of the Swiss Alps, Tectonics, 37, 1097–1115, doi:10.1002/2017TC004762, 2018.

Krayenbuhl, T. and Steck, A.: Structure and kinematics of the Jungfrau syncline, Faflertal (Valais, Alps), and its regional significance, Swiss J. Geosci., 102, 441–456, doi:10.1007/s00015-009-1333-1, 2009.

Labhart, T. P.: Mehrphasige alpine Tektonik am Nordrand des Aarmassivs Beobachtungen im Druckstollen Trift-Speicherberg (Gadmental) der Kraftwerke Oberhaslo AG, Eclogae Geol. Helv., 59, 803–830, doi:doi.org/10.5169/seals-163395, 1966.

Labhart, T. (1977): Aarmassiv und Gotthardmassiv. - Sammlung geolog. Führer Nr. 63, Gebr. Bornträger, Berlin, Stuttgart, 1977.

Lünsdorf, N. K. and Lünsdorf, J. O.: Evaluating Raman spectra of carbonaceous matter by automated, iterative curve-fitting, Int. J. Coal Geol., 160–161, 51–62, doi:10.1016/j.coal.2016.04.008, 2016.

Lünsdorf, N. K., Dunkl, I., Schmidt, B. C., Rantitsch, G. and von Eynatten, H.: Towards a Higher Comparability of Geothermometric Data obtained by Raman Spectroscopy of Carbonaceous Material. Part I: Evaluation of Biasing Factors, Geostand. Geoanalytical Res., 38, 73–94, doi:10.1111/j.1751-908X.2013.00249.x, 2014.

Lünsdorf, N. K., Dunkl, I., Schmidt, B. C., Rantitsch, G. and von Eynatten, H.: Towards a Higher Comparability of Geothermometric Data Obtained by Raman Spectroscopy of Carbonaceous Material. Part 2: A Revised Geothermometer, Geostand. Geoanalytical Res., 41, 593–612, doi:10.1111/ggr.12178, 2017.

Masson, H., Herb, R., Steck, A.: Helvetic Alps of Western Switzerland, Excusion no. 1. in: Trümpy, R. Geology of Switzerland - a guide book, Part B, Geological Excursions, 109-153. Wepf & Co, 1980.

McClay, K. R.: Glossary of thrust tectonics terms. In K. R. McClay (Ed.), Thrust tectonics (pp. 419–433), London: Chapman and Hall, 1982.

Menkveld, J.W.: Der geologische Bau des Helvetikums der Innerschweiz. Diss. Univ. Bern., 1995.

Menkveld-Gfeller, U., Kempf, O. and Funk, H.: Lithostratigraphic units of the Helvetic Palaeogene: review, new definition, new classification, Swiss J. Geosci., 109, 171–199, doi:10.1007/s00015-016-0217-4, 2016.

Milnes, A. G. and Pfiffner, O. A.: Structural development of the infrahelvetic complex, eastern Switzerland, Eclogae Geol. Helv., 70(1), 83–95, doi:10.5169/seals-164615, 1977.

Niggli, E. and Niggli, C.: Karten der Verbreitung einiger Mineralien der alpidischen Metamorphose in den Schweizer Alpen (Stilpnomelan, Disthen, Sillimanit)., Eclogae Geol. Helv., 58, 335–368, doi:10.5169/seals-163268, 1965.

Oberhänsli, R., Schenker, F. and Mercolli, I.: Indications of Variscan nappe tectonics in the Aar Massif, Schweizerische Mineral. und Petrogr. Mitteilungen, 68, 509–520, doi:10.5169/seals-52086, 1988.

Pfiffner, O. A.: The structure of the Helvetic nappes and its relation to the mechanical stratigraphy, J. Struct. Geol., 15, 511–521, doi:10.1016/0191-8141(93)90145-Z, 1993.

Pfiffner, O.A., Burkhard, M., Hänni, R., Kammer, A., Klligflied, A., Mancktelow, N.S, Menkveld, J.W., Ramsay, J.G., Schmid, S.M. and Zurbriggen, R. Structural Map of the Helvetic Zone of the Swiss Alps, including Vorarlberg (Austria) and Haute Savoie (France), 1:100000. Special Geological Maps, Federal Office of Topography swisstopo, 2011.

Pfiffner, O. A.: Geology of the Alps, 2nd ed., Wiley Blackwell., 2014.

Pollack, H. N. and Chapman, D. S.: On the regional variation of heat flow, geotherms, and lithospheric thickness, Tectonophysics, 38, 279–296, doi:10.1016/0040-1951(77)90215-3, 1977.

Rahiman, T. I. H. and Pettinga, J. R.: Analysis of lineaments and their relationship to Neogene fracturing, SE Viti Levu, Fiji, Geol. Soc. Am. Bull., 120, 1544–1555, doi:10.1130/B26264.1, 2008.

Rolland, Y., Cox, S. F. and Corsini, M.: Constraining deformation stages in brittle–ductile shear zones from combined field mapping and 40Ar/39Ar dating: The structural evolution of the Grimsel Pass area (Aar Massif, Swiss Alps), J. Struct. Geol., 31, 1377–1394, doi:10.1016/j.jsg.2009.08.003, 2009.

Rutishauser, H.: Die quantitative Erfassung von Migmatiten im Aufschlussbereich (Erläutert am Beispiel des Lauterbrunner Kristallins), Schweizerische Mineral. und Petrogr. Mitteilungen, 53, 99–124, doi:10.5169/seals-41375, 1973.

Rutishauser, H.: Flüssige Phasen im migmatitlschen Lauterbrunner-Kristallin (Aarmassiv, Alpen), Geol. Rundschau, 86, 560–571, doi:10.1007/BF01820831, 1974.

Sala, P., Pfiffner, O. A. and Frehner, M.: The Alpstein in three dimensions: fold-and-thrust belt visualization in the Helvetic zone, eastern Switzerland, Swiss J. Geosci., 107, 177–195, doi:10.1007/s00015-014-0168-6, 2014.

Schaltegger, U.: The evolution of the polymetamorphic basement in the Central Alps unravelled by precise U-Pb zircon dating, Contrib. to Mineral. Petrol., 113, 466–478, doi:10.1007/BF00698316, 1993.

Schaltegger, U., Albrecht, J. and Corfu, F.: The Ordovician orogeny in the Alpine basement: constraints from geochronology and geochemistry in the Aar Massif (Central Alps), Schweizerische Mineral. und Petrogr. Mitteilungen, 83, 183–195, doi:10.5169/seals-63144, 2003.

Schlunegger, F. and Kissling, E.: Slab rollback orogeny in the Alps and evolution of the Swiss Molasse basin, Nat. Commun., 6, 1–10, doi:10.1038/ncomms9605, 2015.

Schlunegger, F. and Willett, S.: Spatial and temporal variations in exhumation of the central Swiss Alps and implications for exhumation mechanisms, Geol. Soc. London, Spec. Publ., 154(1), 157–179, doi:10.1144/GSL.SP.1999.154.01.07, 1999.

Schmid, S. M., Fügenschuh, B., Kissling, E. and Schuster, R.: Tectonic map and overall architecture of the Alpine orogen, Eclogae Geol. Helv., 97, 93–117, doi:10.1007/s00015-004-1113-x, 2004.

Schmid, S. M., Pfiffner, O. A., Froitzheim, N., Schönborn, G. and Kissling, E.: Geophysical-geological transect and tectonic evolution of the Swiss-Italian Alps, Tectonics, 15(5), 1036–1064, doi:10.1029/96TC00433, 1996.

Schneeberger, R., De la Varga, M., Egli, D., Berger, A., Kober, F., Wellmann, F. and Herwegh, M.: Methods and uncertainty-estimations of 3D structural modelling in crystalline rocks: A case study, Solid Earth Discuss., 1–23, doi:10.5194/se-2017-47, 2017.

Steck, A.: Die alpidischen Strukturen in den Zentralen Aaregranite des westlichen Aarmassivs, Eclogae Geol. Helv., 61, 19–48, doi:10.5169/seals-163584, 1968.

Steck, A.: Structures de déformations tertiaires dans les Alpes centrales (transversales Aar-Simplon- Ossola), Eclogae Geol. Helv., 77(1), 55–100, ~~doi:~~doi~~.org/~~10.5169/seals-165499, 1984.

Stipp, M., Stünitz, H., Heilbronner, R. and Schmid, S. M.: Dynamic recrystallization of quartz: correlation between natural and experimental conditions, Geol. Soc. London, Spec. Publ., 200(1), 171–190, doi:10.1144/GSL.SP.2001.200.01.11, 2002.

Strasser, A.: Fazielle und sedimentologische Entwicklung des Betlis-Kalkes (Valanginian) im Helvetikum der Zentral- und Ostschweiz, Eclogae Geol. Helv., 75(1), 23, doi:10.5169/seals-165212, 1982.

Ustaszewski, M., Herwegh, M., McClymont, A. F., Pfiffner, O. A., Pickering, R. and Preusser, F.: Unravelling the evolution of an Alpine to post-glacially active fault in the Swiss Alps, J. Struct. Geol., 29(12), 1943–1959, doi:10.1016/j.jsg.2007.09.006, 2007.

Wehrens, P., Berger, A., Peters, M., Spillmann, T. and Herwegh, M.: Deformation at the frictional-viscous transition: Evidence for cycles of fluid-assisted embrittlement and ductile deformation in the granitoid crust, Tectonophysics, 693, 66–84, doi:10.1016/j.tecto.2016.10.022, 2016.

Wehrens, P., Baumberger, R., Berger, A. and Herwegh, M.: How is strain localized in a meta-granitoid, mid-crustal basement section? Spatial distribution of deformation in the central Aar massif (Switzerland), J. Struct. Geol., 94, 47–67, doi:10.1016/j.jsg.2016.11.004, 2017.

Valla, P. G., Rahn, M., Shuster, D. L. and van der Beek, P. A.: Multi-phase late-Neogene exhumation history of the Aar massif, Swiss central Alps, Terra Nov., 28(6), 383–393, doi:10.1111/ter.12231, 2016.

Xu, L., Renner, J., Herwegh, M. and Evans, B.: The effect of dissolved magnesium on creep of calcite II: Transition from diffusion creep to dislocation creep, Contrib. to Mineral. Petrol., 157(3), 339–358, doi:10.1007/s00410-008-0338-5, 2009.